Development of Mathematical Equations for the Simulator Model of the Cessna 421 Aircraft

Douglas A. Elliott

December 1982

DOT/FAA/CT-81/37

U.S. Department of Transportation
Federal Aviation Administration

Technical Center
Atlantic City Airport, N.J. 08405

NOTICE

This document is disseminated under the sponsorship of the Department of Transportation in the interest of information exchange. The United States Government assumes no liability for the contents or use thereof.

The United States Government does not endorse products or manufacturers. Trade or manufacturer's names appear herein solely because they are considered essential to the object of this report.

Technical Report Documentation Page

1. Report No.	2. Government Accession No.	3. Recipient's Catalog No.
DOT/FAA/CT-81/37		

4. Title and Subtitle	5. Report Date
DEVELOPMENT OF MATHEMATICAL EQUATIONS FOR THE SIMULATOR MODEL OF THE CESSNA 421 AIRCRAFT	December 1982
	6. Performing Organization Code
7. Author(s)	8. Performing Organization Report No.
Douglas A. Elliott	DOT/FAA/CT-81-37
9. Performing Organization Name and Address	10. Work Unit No. (TRAIS)
Federal Aviation Administration Technical Center Atlantic City Airport, New Jersey 08405	11. Contract or Grant No. 999-724-960
	13. Type of Report and Period Covered
12. Sponsoring Agency Name and Address Federal Aviation Administration Technical Center Atlantic City Airport, New Jersey 08405	Technical Note
	14. Sponsoring Agency Code

15. Supplementary Notes

16. Abstract

This report provides details of methods used for modifying a flight simulator at the Federal Aviation Administration Technical Center to represent any particular aircraft. Methods are discussed for determining the coefficients and derivatives that define the flight characteristics of an aircraft, using readily available published data. The report includes discussion of the equations of motion, methods for computing aerodynamic derivatives, moment of inertia computations, engine power and thrust computations, control force loading, principles of the phugoid oscillation, and autopilot installation and modes of operation.

17. Key Words	18. Distribution Statement
Flight Simulation Aerodynamic Derivatives Aircraft Equations of Motion Cessna 421 Aircraft	

19. Security Classif. (of this report)	20. Security Classif. (of this page)	21. No. of Pages	22. Price
Unclassified	Unclassified	76	

TABLE OF CONTENTS

LIST OF ILLUSTRATIONS

LIST OF TABLES

INTRODUCTION

PURPOSE.

The purpose of this study was to determine values of the coefficients for converting the simulator to a representation of a Cessna 421 aircraft for use in simulator studies for the Advanced Cockpit Technology program. Examples are given of the data used for this aircraft, and the resulting values of the coefficients and derivatives.

In developing the methods for deriving the coefficients, this report includes discussion of the equations of motion, methods for computing aerodynamic derivatives, moment of inertia computations, engine power and thrust computations, control force loading, principles of the phugoid oscillation, and autopilot installation and modes of operation.

BACKGROUND.

This report provides details of methods used for modifying a flight simulator at the Federal Aviation Administration (FAA) Technical Center to represent any particular aircraft. Methods are discussed for determining the coefficients and derivatives that define the flight characteristics of an aircraft, using readily available published data.

Modifications to the flight simulator were made as part of a program to develop a Flight Simulation Facility under NPD 16-234, project 161-020-110, entitled "Establish Human Factors Cockpit Laboratory." This project had the objective of establishing a flexible test environment for human factors experimentation.

BASIC SIMULATOR RELATIONS

An aircraft simulator is essentially a computer representation of a series of equations of motion. These equations describe the response characteristics of a particular aircraft. As shown in figure 1, the equations receive inputs from the control actions of the pilot, and compute outputs which are the resulting aircraft responses. These outputs become feedbacks to the pilot, which are sensed in several ways:

Initially, control loads react against pilot input motions with forces that vary with airspeed and amount of deflection. The magnitudes of these forces give the pilot important information concerning the amount of control influence that he is applying to the aircraft, and contribute to the "feel" of the aircraft which he senses.

Many of the computed outputs are displayed on cockpit instruments to provide information concerning attitudes, rates, airspeed, and altitude, as in an actual aircraft. Cockpit motion is also an optional response which may be included to provide additional "feel" of the aircraft response. Whether or not motion is used, the instrument displays of attitude remain the same.

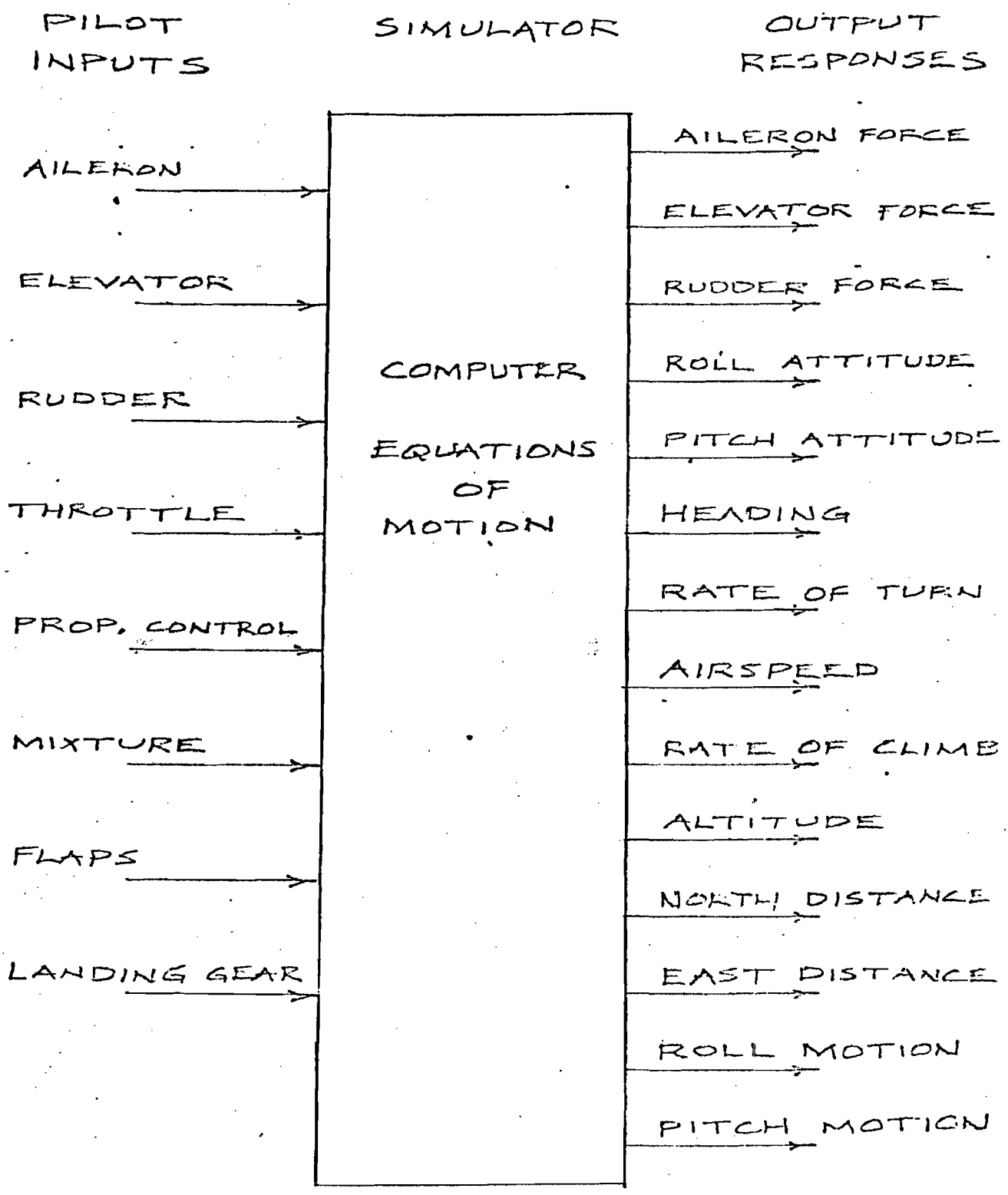

FIGURE 1. BASIC SIMULATOR RELATIONS

In addition to direct displays to the pilot, some of the computer outputs are used in navigation computations. Position data, such as north distance, east distance, and altitude, represent X, Y, and Z locations in the air mass within which the aircraft is flying. These locations become inputs to navigation computations that provide additional cockpit displays showing bearing and distance information relative to navigational aids.

The following sections of this report define the equations that are contained in the simulation computer, including definitions of the nomenclature and numerical values. The methods used, and revised values obtained, for converting the simulator to a representation of a Cessna 421 aircraft are described.

Also included is a discussion of the significance of the phugoid characteristics of an aircraft, and how the coupled loops of the equations of motion produce this type of oscillation. The phugoid characteristics of the Cessna 421 aircraft and the GAT-2 simulator are compared with the analytical computations.

In addition to revisions of the computer equations, representation of the Cessna 421 has required the installation of an autopilot in place of the flight director formerly used. A discussion of the modifications required to install the autopilot is included as well as a detailed description of autopilot operation.

EQUATIONS OF MOTION

AERODYNAMIC EQUATIONS.

The equations which represent the dynamic aircraft response characteristics in the GAT-2 simulator are the six-degree-of-freedom motion equations listed in table 1. The nomenclature used in the equations is defined in table 2. These equations relate the response of the three angular modes and the three translational modes of aircraft motion to pilot inputs.

Figure 2 illustrates the relation of these aircraft motions to the body axis system. The angular modes provide roll, pitch, and yaw accelerations about the aircraft body axes in response to aileron, elevator, and rudder deflections. The translational modes represent the forward, lateral, and vertical accelerations along the aircraft body axes in response to thrust, lift, drag, pitch angle, and bank angle.

In addition, three Euler angle equations are listed in table 1. These equations relate the attitudes of the aircraft body axis system to an earth axis system.

The six equations of aircraft motion are arranged in the form of acceleration responses to force or moment summations. The force and moment terms are expressed in a standard aerodynamic form of generalized dimensionless coefficients and derivatives which is applicable over a wide range of flight conditions and aircraft dimensions.

The following discussion explains the manner in which these equations are organized, and methods for converting the nondimensional coefficients into useful dimensional magnitudes for use in computer simulation.

TABLE 1. EQUATIONS OF MOTION (SHEET 1 OF 3)

ANGULAR MODES

EQ. 1. ROLL ACCELERATION ABOUT LONGITUDINAL BODY AXIS:

$$\dot{p}_a = \frac{q\,S\,b}{I_{xx}}\left[C_{\ell_{\delta_a}}\delta_a + C_{\ell_\beta}\beta + (CG_{lat})C_L + \frac{b}{2u}(C_{\ell_p}p_a)\right]$$

where: $CG_{lat} = \frac{y_1}{b\,W}(W_{t_4} - W_{t_1}) + \frac{y_2}{b\,W}(W_{t_3} - W_{t_2})$

$$C_L = C_{L_o} + C_{L_\alpha}\alpha$$

EQ. 2. PITCH ACCELERATION ABOUT LATERAL BODY AXIS:

$$\dot{q}_a = \frac{q\,S\,\bar{c}}{I_{yy}}\left[C_{m_{\delta_e}}\delta_e + C_{m_{ac}} - (CG_{long})C_L + \frac{\bar{c}}{2u}(C_{m_q}q_a + C_{m_{\dot{\alpha}}}\dot{\alpha})\right]$$

where: $CG_{long} = \frac{x_o - x_{cg}}{\bar{c}}$

EQ. 3. YAW ACCELERATION ABOUT VERTICAL BODY AXIS:

$$\dot{r}_a = \frac{q\,S\,b}{I_{zz}}\left[-C_{n_{\delta_r}}\delta_r + C_L\,C_{n_{\delta_a}}\delta_a + C_{n_\beta}\beta + \frac{b}{2u}(C_{n_r}r_a - C_{n_{\dot{\beta}}}\dot{\beta})\right]$$

For simplicity, minor terms involving asymmetrical thrust, horsepower, landing gear, and flap influences have been omitted from these equations, although they are present in the simulator.

TABLE 1. EQUATIONS OF MOTION (SHEET 2 OF 3)

TRANSLATION MODES

Eq. 4. FORWARD ACCELERATION ALONG LONGITUDINAL AXIS:

$$\dot{u} = \frac{g}{W}\left[\leq T - q\,S\,C_D - W \sin\gamma\right]$$

Eq. 5. LATERAL ACCELERATION ALONG LATERAL BODY AXIS:

$$\dot{v} = \frac{g}{W}\left[q\,S\,C_{y_{\delta_r}}\delta_r - q\,S\,C_{y_\beta}\beta + W \sin\phi\right]$$

EQ. 6. VERTICAL ACCELERATION ALONG VERTICAL AXIS:

$$\dot{w} = -\frac{g}{W}\left[q\,S\,C_L - W\cos\phi + 2.11\,C_L \leq P\right]$$

where: $C_D = C_{D_o} + C_{D_{C_L^2}} C_L^2 + C_{D_\beta}|\beta|$

$C_L = C_{L_o} + C_{L_\alpha}\alpha$

$\dot{\alpha} = q_a - \dot{\gamma}$, in body axes.

$\dot{\beta} = \frac{\dot{v}}{u} - r_a$, in body axes.

$\dot{\gamma} = -\frac{\dot{w}}{u}$, in body axes.

$\gamma = \theta - \alpha\cos\phi$, in earth axes.

FLIGHT PATH ANGLE:

$\tan\gamma = \gamma = -\frac{w}{u}$

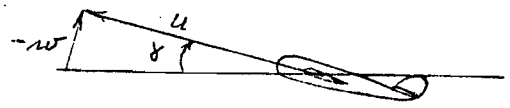

SIDESLIP ANGLE:

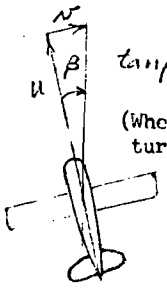

$\tan\beta = \beta = \frac{v}{u}$

(When not turning)

TABLE 1. EQUATIONS OF MOTION (SHEET 3 OF 3)

EULER ANGLE EQUATIONS

EQ. 7. ROLL RATE OF AIRCRAFT BODY AXES RELATED TO EARTH AXES:

$$\dot{\phi} = p_a + \dot{\psi} \sin \theta$$

EQ. 8. PITCH RATE OF AIRCRAFT BODY AXES RELATED TO EARTH AXES:

$$\dot{\theta} = q_a \cos \phi - r_a \sin \phi$$

EQ. 9. YAW RATE OF AIRCRAFT BODY AXES RELATED TO EARTH AXES:

$$\dot{\psi} = r_a \cos \phi + q_a \sin \phi$$

RELATION OF ANGLES AND FORCES TO WING:
(For zero roll angle)

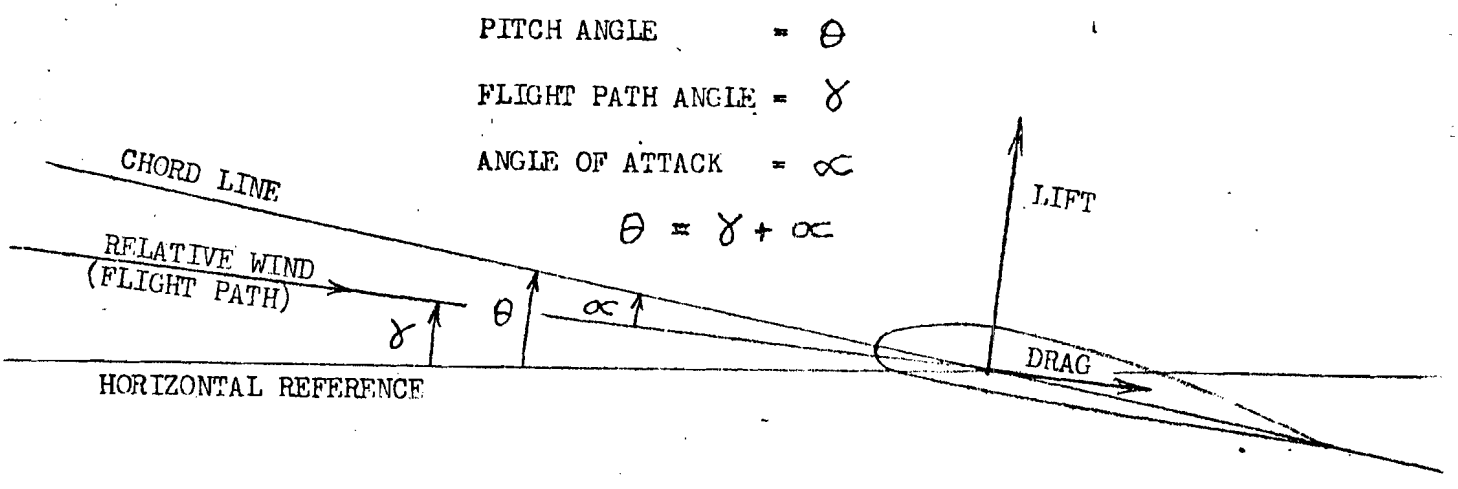

TABLE 2. NOMENCLATURE (SHEET 1 OF 2)

A	Aspect ratio of wing, $b/\bar{c}$, dimensionless.
b	Span of wing, ft.
$\bar{c}$	Average chord of wing, ft.
CG	Center of gravity location, dimensionless ratio.
e	Airplane efficiency factor, dimensionless.
F_x	Longitudinal force, lb, (positive forward).
F_y	Lateral force, lb, (positive right).
F_z	Vertical force, lb, (positive down).
g	Acceleration of gravity, 32.2 ft/sec^2.
h	Altitude, ft.
I_{xx}	Aircraft moment of inertia about longit. axis, slug ft^2.
I_{yy}	Aircraft moment of inertia about lateral axis, slug ft^2.
I_{zz}	Aircraft moment of inertia about vertical axis, slug ft^2.
L	Rolling moment, ft lb, (positive right).
M	Pitching moment, ft lb, (positive nose up).
N	Yawing moment, ft lb, (positive right).
m	Mass of aircraft, W/g, slugs.
P	Brake horsepower of engine.
p_a	Roll rate of rotation about longit. axis, rad/sec, (pos. right).
q_a	Pitch rate of rotation about lateral axis, rad/sec, (pos. up).
r_a	Yaw rate of rotation about vertical axis, rad/sec, (pos. right).
q	Dynamic pressure of air, $\frac{1}{2}\rho u^2$, lb/ft^2.
S	Area of wing, ft^2.
T	Thrust of propeller, lb.
u	Forward velocity of aircraft, True airspeed), ft/sec, (Same as V_p in GAT-2 equations), (positive forward).
v	Lateral velocity of aircraft, ft/sec, (positive right).
w	Vertical velocity of aircraft, ft/sec, (positive down).
W	Gross weight of aircraft, lb.
W_t	Weight of fuel in tank, lb, (subscript denotes tank number).
x_o	Longitudinal distance to aerodynamic center from leading edge of wing, ft.
x_{cg}	Longitudinal distance to center of gravity from leading edge of wing, ft.
y	Lateral distance to center of fuel tank, ft, (subscript denotes tank number).

TABLE 2. NOMENCLATURE (SHEET 2 OF 2)

α	(Alpha)	Angle of attack, radians, (positive nose up).
β	(Beta)	Sideslip angle, radians, (positive, wind from right).
γ	(Gamma)	Flight path angle, radians, (positive nose up).
δ_a	($Delta_a$)	Aileron deflection, (positive right).
δ_e	($Delta_e$)	Elevator deflection, (positive down).
δ_r	($Delta_r$)	Rudder deflection, (positive right).
ρ	(Rho)	Mass density of air, slugs/ft^3.
Σ	(Sigma)	Summation of terms.
ϕ	(Phi)	Roll angle, radians, (positive right).
θ	(Theta)	Pitch angle, radians, (positive nose up).
ψ	(Psi)	Heading (Yaw) angle, radians, (positive right, clockwise).
ω_n	($Omega_n$)	Natural frequency, radians/sec.

A dot above a variable represents the derivative of that variable with respect to time. For example: $\dot{u} = du/dt$, ft/sec^2.

An asterisk applied to a variable represents a normalized magnitude in which unity is full defleotion. For example: $\delta_a^* = -1.0$ represents full left aileron deflection.

Dimensionless force and moment coefficients have the following form:

C_L	Lift coefficient.
C_D	Drag coefficient.
C_y	Lateral force coefficient.
C_l	Rolling moment coefficient.
C_m	Pitching moment coefficient.
C_n	Yawing moment coefficient.

Derivatives of those coefficients are expressed by the addition of a second subscript to define the variable to which the derivative is related. For example: $C_{l_\beta} = dC_l/d\beta$, per radian.

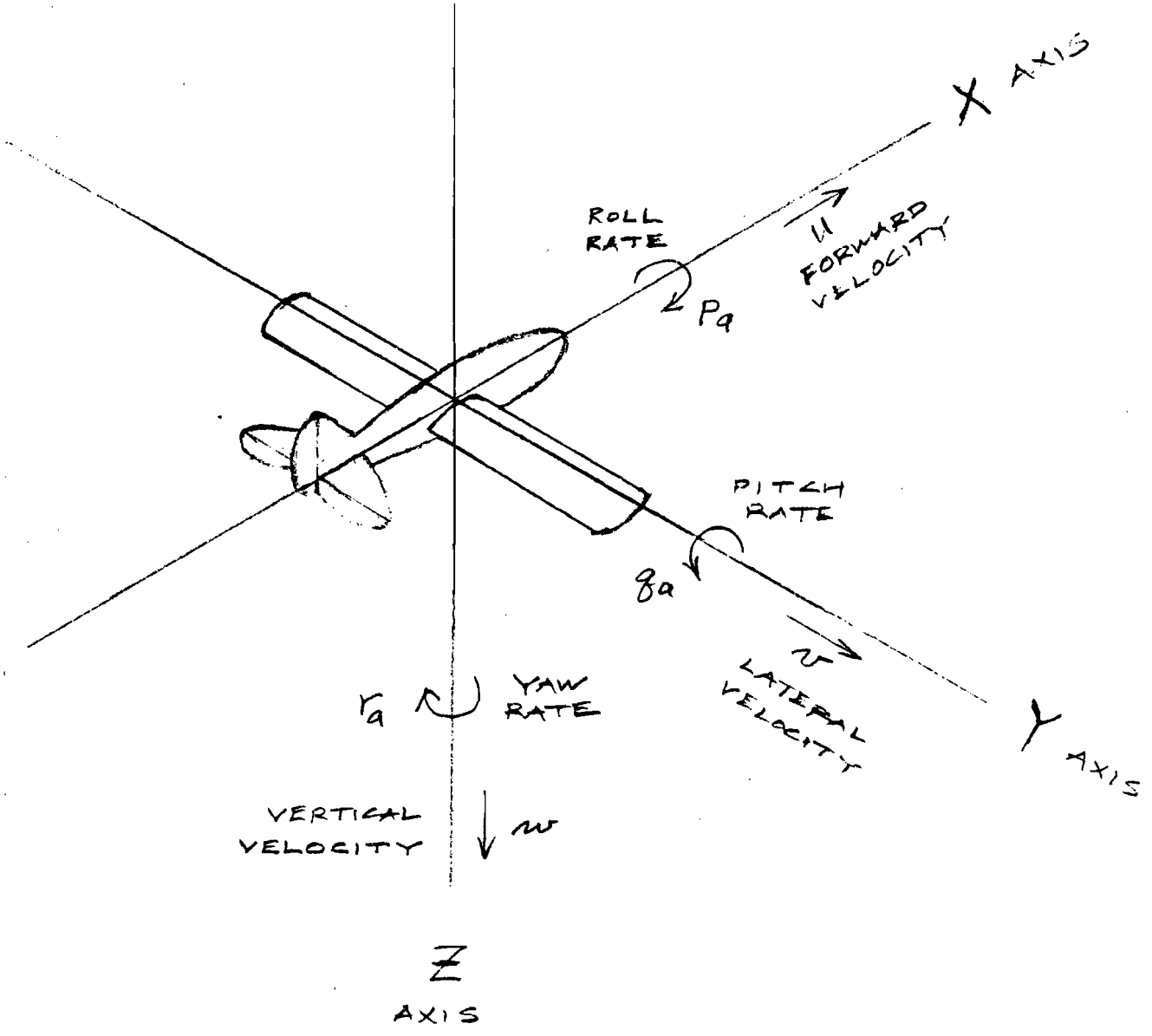

FIGURE 2. AIRCRAFT COORDINATE SYSTEM

TRANSLATION RELATIONS. Motions in translation along each axis result from the influence of summed forces on the corresponding acceleration. This influence is expressed by the basic equation:

mass x acceleration = force summation

From this equation, the relation of translational acceleration to force summation along each axis is:

$$\dot{u} = \frac{g}{W} \Sigma F_x \quad , \quad ft/sec^2$$

$$\dot{v} = \frac{g}{W} \Sigma F_y \quad , \quad ft/sec^2$$

$$\dot{w} = \frac{g}{W} \Sigma F_z \quad , \quad ft/sec^2$$

The resulting accelerations are converted to velocities by time integration operations in the simulator computer.

ROTATION RELATIONS. Motion in rotation about each axis results from the influence of summed moments on the corresponding angular acceleration. This influence is expressed by the basic equation:

moment of inertia x angular accel. = sum of moments

From this equation, the relation of rotational acceleration to moment summation about each axis is:

$$\dot{p}_a = \Sigma L / I_{xx} \quad , \quad rad/sec^2$$

$$\dot{q}_a = \Sigma M / I_{yy} \quad , \quad rad/sec^2$$

$$\dot{r}_a = \Sigma N / I_{zz} \quad , \quad rad/sec^2$$

These accelerations are converted to angular velocities by time integration operations in the simulator computer.

DIMENSIONLESS COEFFICIENTS. In aerodynamic equations, forces and moments are expressed in terms of dimensionless coefficients which are valid over a wide range of airspeeds, altitudes, and aircraft dimensions. These coefficients are converted to actual magnitudes of forces or moments by application of appropriate values of dynamic pressure and aircraft dimensions. The resulting magnitudes then become the force and moment terms in acceleration equations.

In translation, the coefficients are multiplied by a reference force defined by the product of the dynamic pressure, q, acting on the wing area, S. The resulting force relations in translation along the three aircraft axes are expressed as:

$$\text{Vertical force:} \quad \text{LIFT} = q\,S\,C_L \text{ , lb.}$$

$$\text{Longitudinal force:} \quad \text{DRAG} = q\,S\,C_D \text{ , lb.}$$

$$\text{Lateral force:} \quad F_y = q\,S\,C_y \text{ , lb.}$$

In rotation, the coefficients are multiplied by a reference moment. This moment is defined by the product of a linear dimension and the force reference, qS, used in translation. For pitch, the linear dimension is the wing chord. For roll and yaw, the linear dimension is the wing span. The resulting moment relations about the three aircraft axes are:

$$\text{Rolling moment:} \quad L = q\,S\,b\,C_{\ell} \text{ , ft-lb.}$$

$$\text{Pitching moment:} \quad M = q\,S\,\bar{c}\,C_m \text{ , ft-lb.}$$

$$\text{Yawing moment:} \quad N = q\,S\,b\,C_n \text{ , ft-lb.}$$

DERIVATIVES OF COEFFICIENTS. Derivatives of the dimensionless coefficients are used to represent variations of the coefficients caused by other variables. These derivatives then have the dimensions of the influencing variables as denominator terms. The derivatives are expressed in a shorthand notation in which a second subscript represents the influencing variable. An example is the variation of the lift coefficient caused by variation of the angle of attack. This derivative is expressed as:

$$C_{L_\alpha} = \frac{dC_L}{d\alpha} \text{ , per radian.}$$

Applying dimensions to the derivative, the component of lift resulting from angle of attack becomes:

$$\text{LIFT}_\alpha = q\,S\,C_{L_\alpha}\,\alpha \text{ , lb.}$$

For moment coefficients, the derivatives are expressed by the addition of a second subscript in the same manner as the force derivatives. For example, the variation of the yawing moment resulting from sideslip angle is:

$$C_{n_\beta} = \frac{dC_n}{d\beta} \quad , \quad \text{per radian.}$$

In dimensional form, the component of yawing moment resulting from sideslip angle is:

$$N_\beta = q\ S\ b\ C_{n_\beta}\beta \quad , \quad \text{ft-lb.}$$

When moment coefficients are related to angular rates, as in the case of damping feedback terms, additional dimensions are used to cancel the time dimension of the rate. These dimensions include half of the wing span or chord, and the forward velocity of the aircraft. When combined with the angular rates, the following nondimensional parameters are formed:

$$\text{Non-dimensional roll rate} = \frac{p_a b}{2u}$$

$$\text{Non-dimensional pitch rate} = \frac{q_a \bar{c}}{2u}$$

$$\text{Non-dmensional yaw rate} = \frac{r_a b}{2u}$$

An example is the derivative of rolling moment coefficient with respect to angular rate:

$$C_{l_p} = \frac{dC_l}{d\left(\frac{p_a b}{2u}\right)}$$

In dimensional form, a component of rolling moment resulting from roll rate is expressed as:

$$\frac{dL}{dp_a} = q\,S\,b\left(\frac{b}{2u}\right)C_{\ell_p}\ ,\ \frac{\text{ft-lb}}{\text{rad/sec}}$$

DISCUSSION OF EQUATIONS. The six equations of motion which are presented in table 1 include the major terms that determine the response characteristics of the aircraft. Some minor terms that are present in the GAT-2 simulator have been omitted from this table to simplify the presentation. Such terms involve the influences of landing gear or flap extension, and asymmetrical thrust, that have the effect of external disturbances but do not affect the dynamic response characteristics of the aircraft. These terms have been left unchanged in the Cessna 421 simulation.

These are not linearized equations which show only small variations about an equilibrium point, but are general equations which describe the aircraft response characteristics over the full range of flight conditions. The equations include steady-state equilibrium conditions, as well as dynamic variations. Terms such as q, u, W, and C_L are variables, in addition to the normal variables that are associated with each derivative.

The meaning of each term that appears in the six equations is examined in the following discussion.

Angular Equations. Each equation of rotational motion shows the basic form of an angular acceleration equal to a summation of moments divided by the appropriate moment of inertia. The dimensionalizing terms have been factored out so that the summation of terms within the brackets is expressed in coefficient and derivative form.

Roll. Equation 1 shows that the summation of rolling moments includes the influence of aileron deflection, the effect of sideslip angle acting on the dihedral angle of the wing, the effect of lateral displacement of the center of gravity, and a damping term opposing roll rate.

The lateral center of gravity term results from uneven distribution of fuel in the wing tanks. An auxiliary equation for this term utilizes values of fuel weight in each tank to determine an offset center of gravity distance as a fraction of the wing span. Lift of the wing, acting at the centerline of the aircraft, provides a rolling moment in proportion to the center of gravity distance.

A second auxiliary equation shows that the lift coefficient is the sum of a constant term plus a derivative term that varies with angle of attack. For simplicity, the effect of wing stall at high angle of attack, which is present in the simulator, has been omitted from these equations.

In the steady state, an aileron trim deflection must be applied to oppose any sideslip angle or lateral offset of center of gravity. The moment summation then becomes zero with no roll rate.

Pitch. Equation 2 shows a summation of pitching moments which includes the influence of elevator deflection; a constant coefficient of moment about the wing aerodynamic center, which is a characteristic of the airfoil; the effect of the longitudinal location of the center of gravity; and damping terms opposing pitch rate and rate of change of angle of attack.

An auxiliary equation expresses the longitudinal location of the center of gravity, relative to the aerodynamic center, as a fraction of the wing chord. Lift of the wing, acting at the aerodynamic center, provides a pitching moment proportional to the distance to the center of gravity. The lift coefficient equation listed with the roll equation also applies to this case.

In the steady state, the initial moment about the aerodynamic center and the effect of center of gravity must be balanced by elevator deflection so that the moment summation becomes zero.

Yaw. Equation 3 shows a summation of yawing moments that includes the effect of rudder deflection, the adverse yaw effect of aileron deflection, the restoring influence of sideslip angle, and damping moments that oppose yaw rate and rate of change of sideslip angle.

No steady-state unbalanced moment is shown. Any inequality of power between the two engines will produce an external input moment of unbalanced thrust which must be opposed by rudder deflection.

Translational Equations. Each equation of translational motion shows the basic form of a linear acceleration equal to a summation of forces divided by the mass of the aircraft, with mass expressed as W/g. Dimensionalizing terms have not been factored out, and each term in the summation is expressed as a force.

Auxiliary equations are also shown that represent interactions among the equations of motion. The drag coefficient is shown as the sum of a constant term, plus terms that vary with lift coefficient and the absolute magnitude of sideslip angle. The lift coefficient relation is the same as that discussed under the roll equation. Expressions are also shown for interactions that produce angle of attack, sideslip angle, and flight path angle. The influence of these and other interaction effects is covered later in a discussion of the significance of coupling among the equations of motion.

Forward Motion. Equation 4 shows a summation of longitudinal forces which includes the total thrust of two propellers, the drag of the aircraft, and the longitudinal component of gross weight when the flight path is inclined upward in a climb or downward in a descent. The drag term has the effect of a damping feedback since the magnitude of the drag varies in relation to forward velocity, as expressed by the dynamic pressure, q.

Steady-state equilibrium of this equation will occur when the forward speed increases or decreases to a magnitude at which the drag force is equal and opposite to the combined effects of thrust and longitudinal weight component.

Lateral Motion. Equation 5 shows a summation of lateral forces which includes a sideward force produced by rudder deflection, a damping force resulting from sideslip angle, and a lateral component of gross weight resulting from bank angle.

In the steady-state level flight condition, all terms are zero in this force summation. In turning flight, the bank angle must be sufficient to cause the weight component to produce a lateral acceleration equivalent to the yawing rate, as expressed in the auxiliary equation for sideslip angular rate.

Vertical Motion. Equation 6 is shown as a negative response to a force summation. This results from the definition of vertical translation as positive downward. The principal vertical force terms are lift of the wing and gross weight of the aircraft. A secondary term reflects the increase in lift caused by propeller slipstream over the wing in relation to engine power.

In the steady-state condition, equilibrium occurs when the lift terms equal the component of weight along the vertical axis. When the aircraft is banked, the weight component is reduced in accordance with the cosine of the bank angle.

Simplifications. Although lift and drag are normally defined as forces perpendicular and parallel to the relative wind, they are shown in the simulator equations as parallel to the vertical and longitudinal axes. This simplifies the equations and causes negligible error. The angle of incidence at which the wing is attached to the fuselage is approximately equal to the angle of attack at cruising conditions. In this case, the relative wind is aligned with the longitudinal axis, and the simplification is correct. At angles of attack greater or less than the angle of incidence, the accuracy of the approximation is indicated by the cosine of the angular difference. This angle will normally be no greater than 5 degrees, which results in a value of 0.996 for the cosine. This indicates that the application of lift and drag along the body axes is better than 99 percent accurate under most flight conditions.

Thrust is also expressed as a force parallel to the longitudinal axis, in opposition to drag. The component of thrust opposing drag depends upon the cosine of the angle between the thrust line and the relative wind. This angle will normally not exceed 5 degrees, which provides an accuracy better than 99 percent when applied along the longitudinal axis. A vertical component of thrust parallel to the lift force is also present. This component depends upon the sine of the same angle. For angles of less than 5 degrees, the component is less than one-tenth of the thrust. Since the thrust is equal to drag, which is less than one-tenth of the lift, omission of the vertical thrust component represents an error of less than 1 percent of the lift magnitude.

Coupling of Equations. The six equations of motion are shown as six individual independent relations in table 1. Actually, these expressions are only portions of coupled dynamic equations which interconnect all of the aircraft motions in a series of feedback loops. The six equations represent the summing junctions of the complete dynamic relations. Couplings among the equations are provided by the Euler angle equations and by the angle of attack, sideslip angle, and flight path angle expressions.

The block diagrams of figures 3 and 4 illustrate the coupled equations. Time integrations at appropriate points provide the conversions between accelerations, velocities, and positions. These integrations cause the time responses that transform the equations of motion into dynamic simulations of aircraft response characteristics. The block diagrams represent the analog computer relations that are used to mechanize the equations of motion.

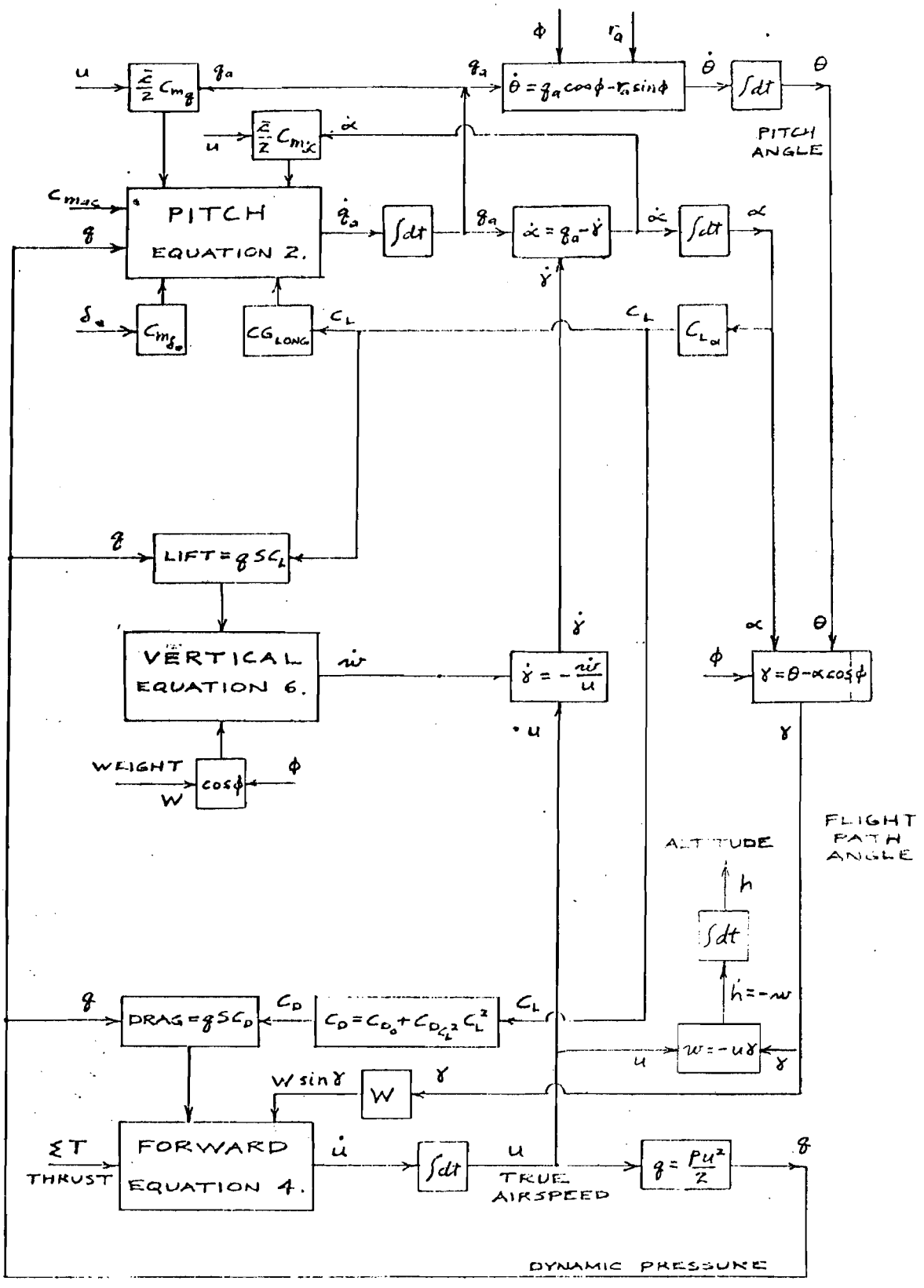

FIGURE 3. PITCH, VERTICAL, AND FORWARD EQUATIONS

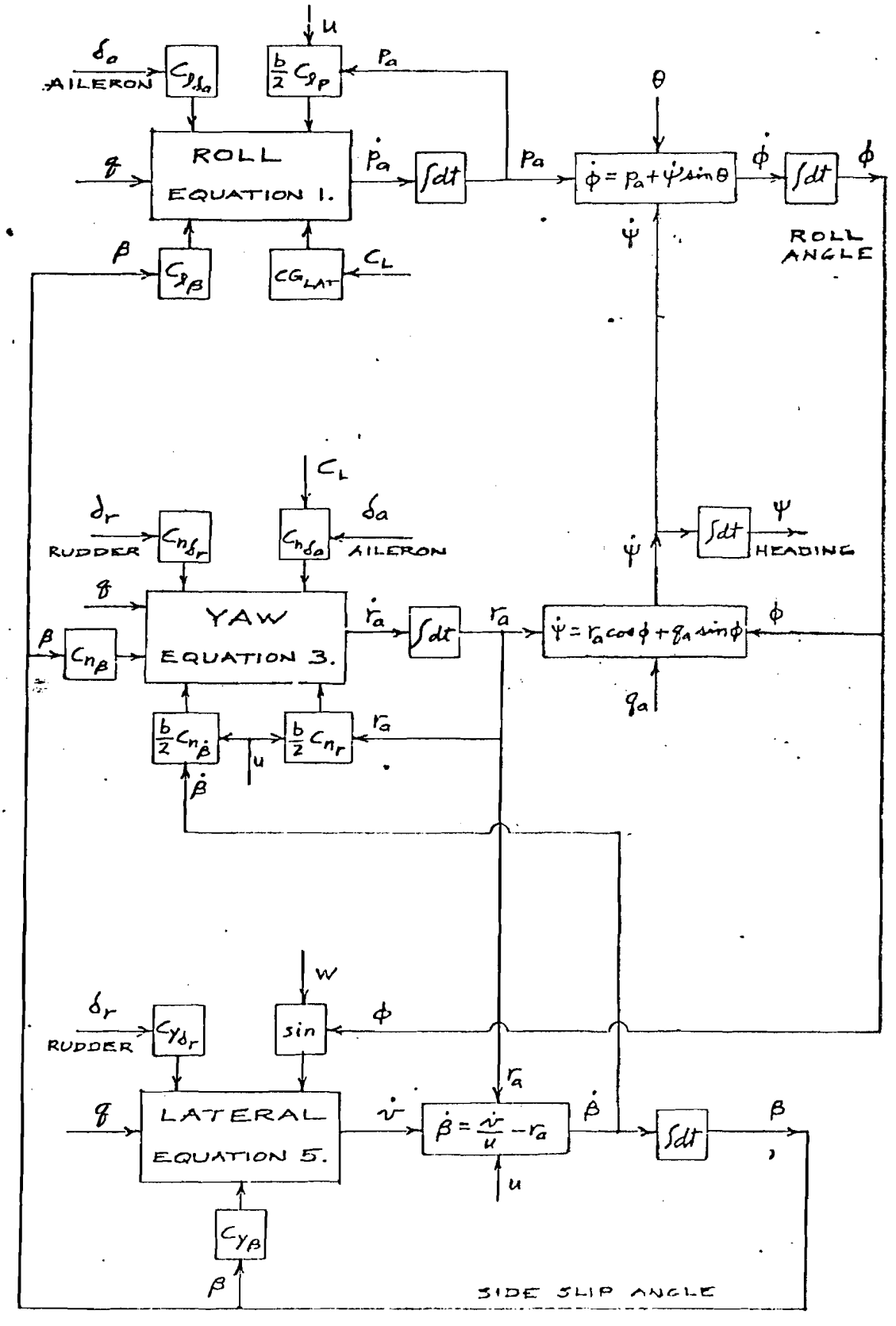

FIGURE 4. ROLL, LATERAL, AND YAW EQUATIONS

The longitudinal coupled equations produce the phugoid oscillation in which energy is interchanged between airspeed and altitude. A discussion of the mathematical relations involved in this oscillation is presented in appendix D.

NUMERICAL VALUES.

Aircraft dimensions obtained from three-view drawings for both the Cessna 310, which was represented by the original GAT-2 configuration, and the Cessna 421, to which the simulator has been revised, are presented in table 3.

Values of the aerodynamic coefficients and derivatives are sometimes available from the aircraft manufacturer, and are the result of computations, wind tunnel tests, or flight tests. When such data are not available, values can be calculated with sufficient accuracy for simulation purposes by using airfoil data and aircraft dimensions in accordance with methods described in textbooks such as "Airplane Performance Stability and Control" by Perkins and Hage, or "Dynamics of Flight" by Bernard Etkin.

Revised values of the aerodynamic derivatives for the Cessna 421 have been determined by calculations using the Perkins and Hage methods. Appendix A presents details of the methods used. The results are listed in table 4, which compares the computed Cessna 421 values with the original values used in the GAT-2 simulator as a representation of the Cessna 310. Appendix B discusses a method for determining moment of inertia values.

The characteristics of the two aircraft are sufficiently similar so that many of the Cessna 421 values are not significantly different from the original GAT-2 values. This is particularly true of terms involving angular accelerations and velocities which affect only initial dynamic response to control motions. For the type of study in which the Cessna 421 simulation will be used, which principally involves navigation and cruising conditions, steady-state equilibrium relations require more accurate simulation than dynamic characteristics.

Significant differences do exist between the Cessna 421 and the Cessna 310 in steady-state performance characteristics. Determination of revised values for these terms has received the major emphasis in revising the GAT-2 simulation. These modifications have involved principally: engine power relations, thrust and drag characteristics for performance matching, and control force relations. The discussions which follow describe analytical methods that have been used to determine revised coefficients for these functions, and provide a comparison between the original and revised values.

Appendix C presents a discussion of the methods used to modify the GAT-2 analog computer to incorporate the revised coefficient values that have been computed for the Cessna 421.

ENGINE POWER, THRUST, AND DRAG

In addition to the basic equations of motion, there are significant relations that act as forcing function inputs to the longitudinal equation of motion. These are the engine power and propeller thrust characteristics that provide forward force

TABLE 3. AIRCRAFT DIMENSIONS AND VALUES

		CESSNA 310 (original GAT-2)	CESSNA 421 (at max. W, 18% CG)
b	ft	37.0	41.8
$\bar{c}$	ft	4.83	5.05
S	ft^2	178.7	211.2
W	lb	5200	7450
I_{xx}	slug ft^2	7800	7123
I_{yy}	slug ft^2	1920	7659
I_{zz}	slug ft^2	9850	13110

TABLE 4. COEFFICIENT AND DERIVATIVE VALUES

	ORIGINAL GAT-2	CESSNA 421
C_{L_o}	0.077	0.100
C_{L_α}	4.57	4.85
C_{D_o}	0.026	0.029
$C_{D_{C_L^2}}$	0.0625	0.0597
C_{D_β}	0.1719	0.1719
$C_{y_{\delta_r}}$	0.1152	0.1449
C_{y_β}	-0.6962	-0.8633
$C_{\ell_{\delta_a}}$	-0.0859	-0.0696
C_{ℓ_β}	-0.1014	-0.0600
C_{ℓ_p}	-0.5487	-0.5300
$C_{m_{ac}}$	-0.0144	-0.0150
$C_{m_{\delta_e}}$	-2.1360	-1.901
C_{m_q}	-57.30	-28.58
$C_{m_{\dot{\alpha}}}$	-57.30	-9.69
$C_{n_{\delta_r}}$	-0.1152	-0.1153
$C_{n_{\delta_a}}$	0.0301	0.0301
C_{n_β}	0.1444	0.1860
$C_{n_{\dot{\beta}}}$	0.0776	0.0040
C_{n_r}	-0.1786	-0.14

Dimensions are per radian.

in opposition to drag so that flying speed is produced. Aircraft performance characteristics, such as airspeed, climb, and descent responses depend upon accurate simulation of these relations.

The following discussions describe the methods used to compute values of these terms which will provide a suitable simulation of Cessna 421 characteristics.

HORSEPOWER.

The original GAT-2 equation for engine brake-horsepower is of the form:

$$BHP = C_1 + C_2N + C_3MAP + C_4h + C_5\Delta T_k$$

where: N = engine speed, rpm.

MAP = manifold absolute pressure, in. Hg.

h = altitude, feet.

ΔT_k = temperature difference from standard, deg. Kelvin.

In the case of the Cessna 421, the engines are equipped with turbo-superchargers which have automatic controls. For fixed throttle and rpm settings, these controls compensate for altitude variations so as to maintain constant manifold pressure and horsepower up to an altitude of approximately 20,000 feet. Figure 5 illustrates the Cessna 421 power characteristics related to manifold pressure, rpm, and altitude. For this aircraft, propeller rpm instead of engine rpm is the speed reference.

Using standard temperatures, and with the altitude term eliminated by the supercharger, the horsepower equation is reduced to the following simplified form for the Cessna 421:

$$BHP = C_1 + C_2N_p + C_3MAP$$

where: N_p = propeller speed, rpm.

$N/N_p = 1.5$, propeller gear ratio.

This expression defines the horsepower relation below 20,000 feet at standard temperatures. Equations for decreasing horsepower at higher altitudes have not been included, since the test program will use altitudes below this level.

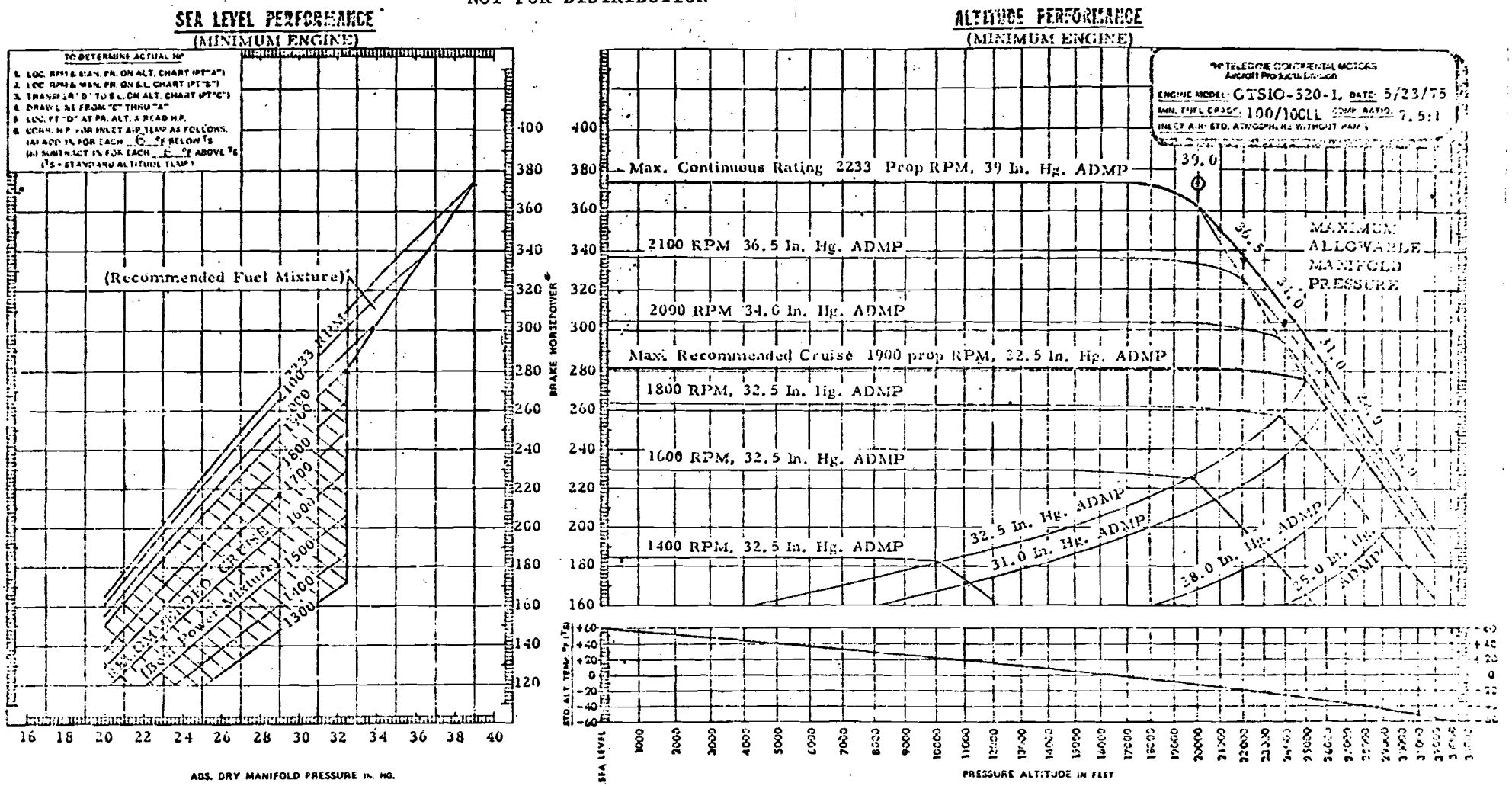

* Horsepower obtained with 6.0 In. H_2O cooling air pressure drop across intercooler except for max. continuous rating which is with 3.5 In. H_2O cooling air pressure drop.

⊙39 In. Hg. ADMP, 2233 RPM, 6 In. H_2O cooling air pressure drop across intercooler.

FIGURE 5. CESSNA 421 ENGINE POWER RELATIONS

Revised values for the three coefficients in the reduced horsepower equation have been calculated to match the Cessna 421 engine power curves in the cruise power region. The area from 1600 to 1900 rpm and from 23.0 to 32.5 in. Hg has been selected as the region where closest matching is desired. Four power conditions have been chosen to cover the desired range. Solutions for the three coefficients are obtained by solving simultaneous equations for various combinations of three conditions at a time, and averaging the results. The power conditions used for these solutions are:

N_p, rpm	MAP, in. Hg	BHP
1900	32.5	280
1900	25.0	208
1800	23.0	173
1600	32.5	230

The resulting equation is:

$$BHP = -323 + 0.1533\ N_p + 9.58\ MAP$$

This linear equation provides good accuracy for cruise powers. At propeller speeds above 2000 rpm, the equation provides somewhat higher power than the nonlinear engine power curves.

PROPELLER SPEED.

GOVERNOR CONTROL. For the Cessna 421, the governing range of the propeller speed control extends from 1300 rpm to 2275 rpm, as the propeller control lever is moved between minimum and maximum positions. The GAT-2 equation for the governed regime of propeller speed has been modified to the following values to represent the Cessna 421 range:

$$N_p = 1300 + 975\ \delta^*_{pc}$$

where: δ^*_{pc} is propeller control position, 0 = minimum, 1.0 = maximum.

UNGOVERNED PROPELLER SPEED. In the ungoverned regime, when the propeller blade angle is at the low-pitch stop, as in static or taxiing conditions, propeller speed varies in relation to throttle position. The GAT-2 equation for this regime has been modified to achieve the following objectives for the case of the Cessna 421 at zero airspeed: at the minimum throttle position, idling speed will be 550 rpm; at the full throttle position, a speed equal to the maximum governor setting of 2275 rpm will be reached. The resulting equation for the Cessna 421 in the ungoverned case is:

$$N_p = 2150 + 50\ \delta^*_{ml} + 75\ \delta^*_{mr} + (6.3\ V_i - 1725)(1 - \delta^*_{th})^2$$

where: δ^*_{ml} is left magneto, 0 = off, 1.0 = on.

δ^*_{mr} is right magneto, 0 = off, 1.0 = on.

δ^*_{th} is throttle position, 0 = min., 1.0 = max.

V_i is indicated airspeed, ft/sec.

The computer circuitry of the GAT-2 simulator selects the lesser of the governed or ungoverned speed computations as the value to be used in the power equations.

MANIFOLD ABSOLUTE PRESSURE (MAP).

With turbo-superchargers, the engines in the Cessna 421 are capable of developing manifold pressures in excess of atmospheric pressure. At the maximum speed of 2275 rpm, a manifold pressure of 39.5 in. Hg produces the maximum rated power of 385 horsepower per engine.

For the Cessna 421 simulation, the GAT-2 equation relating MAP to throttle position has been modified so that increasing engine speed produces a positive increase of manifold pressure at full throttle. Variation of altitude up to 20,000 feet does not influence the manifold pressure. The revised equation is:

$$MAP = 29.92 + 0.0048\ N_p - 0.025\ (1 - \delta^*_{th})^2\ N_p$$

This equation is illustrated graphically in figure 6.

At 2275 rpm, the equation produces a maximum manifold pressure of 40.8 in. Hg, which is above the permissible value of 39.5 in. Hg. This excess pressure has been selected so that the pilot workload will include the task of properly setting the throttles for the maximum permissible manifold pressure. At all other power settings, the full throttle manifold pressure capabilities are above the engine limit values, so that part-throttle settings are required for all power conditions.

At the closed-throttle end of the range, the slope of MAP vs. RPM has been selected to produce negative horsepower values that create adequate windmilling drag. The amount of negative horsepower has been selected to provide deceleration and descent performance that corresponds to Cessna 421 data.

CESSNA 421 MANIFOLD PRESSURE RELATION

$$MAP = 29.92 + 0.0048\ N_p - 0.025\ (1 - \delta^*_{th})^2\ N_p$$

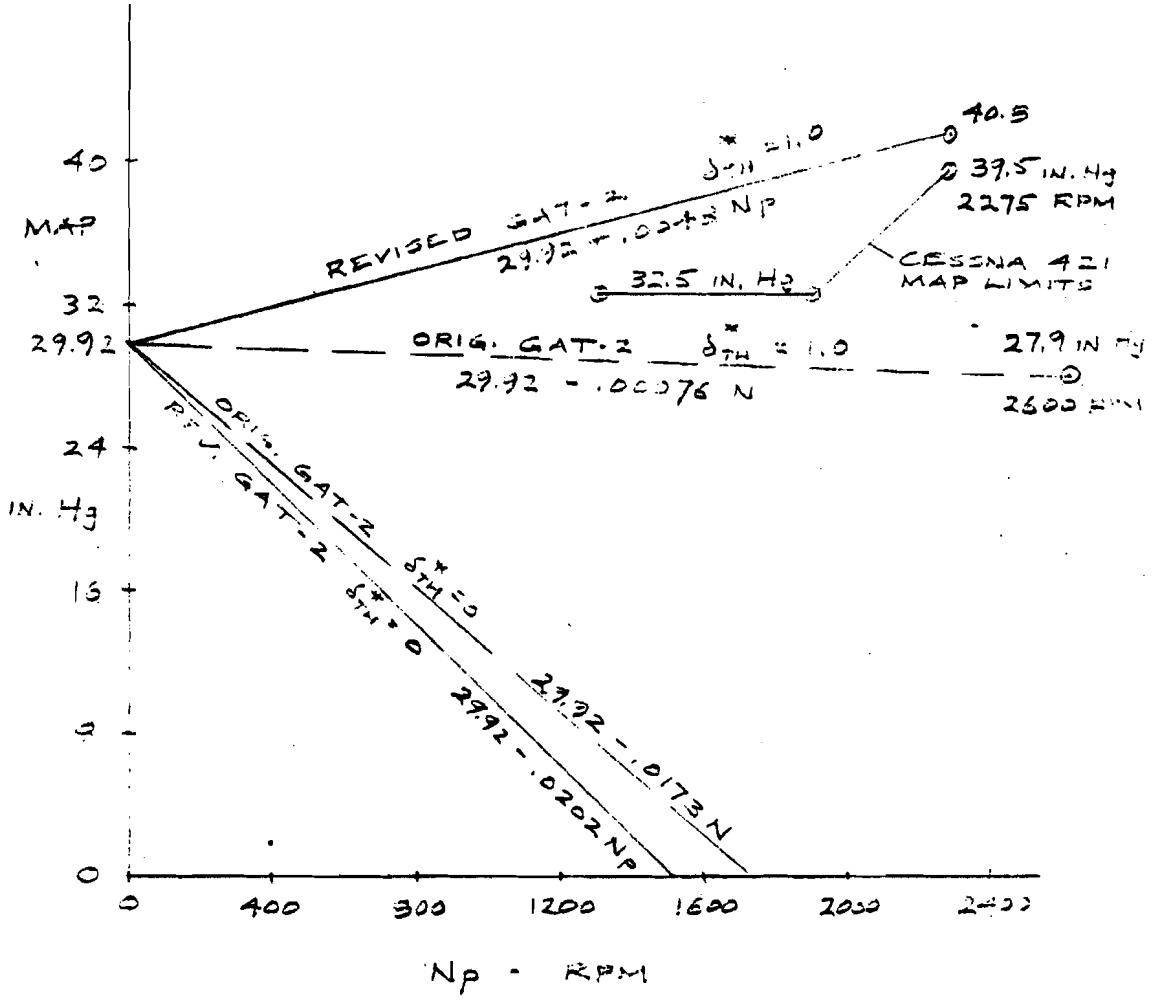

FIGURE 6. MANIFOLD PRESSURE RELATIONS TO MATCH CESSNA 421

SUMMARY OF POWER EQUATIONS.

Table 5 presents a summary of the modified GAT-2 equations which represent the Cessna 421 horsepower, propeller speed, and manifold pressure relations. For comparison, this table also lists the original GAT-2 equations which correspond to Cessna 310 characteristics before modification.

THRUST AND DRAG RELATIONS.

Coefficients for thrust and drag equations have been computed from data obtained from Cessna 421 performance charts. Sea level conditions have been used so that airspeed can be normalized as indicated airspeed. The GAT-2 thrust and drag expressions then appear in the following form:

$$\text{THRUST:} \quad T_n = (K_1 - K_2 V_i)\ \text{BHP} \quad , \quad \text{Per engine.}$$

$$\text{DRAG:} \quad F_{xa} = -qS(K_3 + K_4 C_L^2)$$

$$\text{where:} \quad q = \rho_o V_i^2/2 = 0.001189\ V_i^2$$

$$C_L = W/qS = 34.65/q$$

For equilibrium level flight conditions, where drag equals the thrust of two engines, these relations are equated to one expression:

$$2(K_1 - K_2 V_i)\ \text{BHP} = qS(K_3 + K_4 C_L^2)$$

Selecting values of BHP and V_i at four flight conditions permits the solution of four simultaneous equations to obtain values for the four coefficients. The results of a large number of flight conditions have been averaged to obtain the values used to represent the Cessna 421 in the simulator equations. The altitude terms have not been changed from the original GAT-2 values. The resulting Cessna 421 equations, compared with the original GAT-2 expressions (for Cessna 310) are shown in table 6.

Using these equations, the performance of the simulator is in good agreement with the Cessna 421 cruise performance tables at all altitudes up to 20,000 feet.

FUEL FLOW AND FUEL PRESSURE.

Values of fuel flow for lean mixture, defined by cruise performance charts for the Cessna 421 aircraft, follow a linear relationship which is expressed by the equation:

$$W_f = 10 + 0.403\ \text{BHP}$$

TABLE 5. SUMMARY OF REVISED POWER EQUATIONS

BRAKE HORSEPOWER:

ORIG.: $BHP = -352 + 0.1155\,N + 10.8\,MAP + 0.0025\,h - 0.32\,\Delta T_k$

C-421: $BHP = -323 + 0.1533\,N_p + 9.58\,MAP - 0.32\,\Delta T_k$

SPEED IN GOVERNING RANGE, RPM:

ORIG.: $N = 1650 + 950\,\delta^*_{pc}$

C-421: $N_p = 1300 + 975\,\delta^*_{pc}$

SPEED BELOW GOVERNING RANGE, RPM:

ORIG.: $N = 2500 + 50\,\delta^*_{ml} + 75\,\delta^*_{mr} + (6.3V_i - 2075)(1 - \delta^*_{th})^2$

C-421: $N_p = 2150 + 50\,\delta^*_{ml} + 75\,\delta^*_{mr} + (6.3V_i - 1725)(1 - \delta^*_{th})^2$

MANIFOLD ABSOLUTE PRESSURE, in. Hg:

ORIG.: $MAP = 29.92 - 0.00076\,N - 0.0009\,h - 0.0165(1 - \delta^*_{th})^2\,N$

C-421: $MAP = 29.92 + 0.00480\,N_p - 0.025(1 - \delta^*_{th})^2\,N_p$

where: h = Altitude, ft

ΔT_k = Temperature difference from standard, deg. K

δ^*_{ml} = Left magneto. On = 1.0 , off = 0

δ^*_{mr} = Right magneto. On = 1.0 , off = 0

δ^*_{pc} = Propeller control. Max. = 1.0 , min. = 0

δ^*_{th} = Throttle. Max. = 1.0 , min. = 0

N = Engine speed, RPM

N_p = Propeller speed, RPM , ($N/N_p = 1.5$)

(Equations valid below 20,000 ft altitude).

TABLE 6. REVISED THRUST AND DRAG RELATIONS

THRUST, LB. PER ENGINE:

ORIG.: $T_n = (3.50 - 0.00642 V_i - 0.0000473 h + 0.869 \times 10^{-7} V_i h)$ BHP

C-421: $T_n = (3.58 - 0.0068 V_i - 0.0000473 h + 0.869 \times 10^{-7} V_i h)$ BHP

DRAG, LB.

ORIG.: $F_{x_a} = -179 q (0.026 + 0.0625 C_L^2)$

C-421: $F_{x_a} = -215 q (0.029 + 0.0597 C_L^2)$

where: T_n = Net thrust per engine, lb.

V_i = Indicated airspeed, ft/sec.

BHP = Brake horsepower per engine.

F_{x_a} = Longit. aerodynamic force, lb, = $- Sq(C_D)$

For the maximum rated takeoff power of 385 BHP, this equation provides a fuel flow value of 165 lb/hr (at lean mixture). The rich mixture fuel flow for this power condition is 255 lb/hr, which indicates a variation of 90 lb/hr between rich and lean mixture conditions. Assuming that the mixture control lever is scaled to provide cruising lean mixture at the midpoint of its travel, full stroke of the lever then provides a variation of 180 lb/hr. The resulting fuel flow relation, which includes the effects of both horsepower and mixture, is defined by the following equation:

$$W_f = -80 + 180\ \delta^*_{mix} + 0.403\ BHP$$

where: W_f = fuel flow, lb/hr

BHP = brake horsepower

δ^*_{mix} = mixture control, 0 = off, 1.0 = rich.

A fuel pressure instrument, provided for each engine, indicates a pressure proportional to fuel flow. Markings on the instrument face have been correlated with Cessna 421 fuel flow conditions by using the following equivalent values:

Power (%)	Mixture	Fuel Flow (lb/hr)	Fuel Pressure (psi)
100	Rich	255	17
75	Cruise Lean	125	9
65	Cruise Lean	110	8
55	Cruise Lean	95	7
45	Cruise Lean	80	6

The expression that relates fuel pressure to fuel flow with suitable accuracy is:

$$P_f = 0.07\ W_f$$

Where: P_p is fuel pressure, lb/in^2

A summary of the revised fuel flow and fuel pressure relations, compared with the original GAT-2 equations, is presented in table 7.

TABLE 7. FUEL FLOW AND FUEL PRESSURE

FUEL FLOW, LB/HR:

ORIG.: $W_f = 18 + 18 \left(\delta^*_{mix} - 1 \right) + 0.425 \text{ BHP}$

C-421: $W_f = 100 + 180 \left(\delta^*_{mix} - 1 \right) + 0.403 \text{ BHP}$

FUEL PRESSURE, PSI:

ORIG.: $P_f = 0.118 W_f$

C-421: $P_f = 0.070 W_f$

where: W_f = Fuel weight flow, lb/hr per engine.

P_f = Fuel pressure, lb/in^2.

δ^*_{mix} = Mixture control, 1.0 = rich, 0 = off.

CONTROL FORCE LOADING.

Some of the most significant influences that represent the characteristics of a particular aircraft are the resisting forces that are felt by a pilot as he moves the controls. These forces provide important sensory feedbacks which indicate how much control effect the pilot is producing as he moves control surfaces, such as elevators or ailerons. The forces result from both the amount of deflection and the airspeed. At high airspeed, a smaller deflection is required to develop a given force than at low airspeed. The effectiveness of a control surface in applying moment to the aircraft is directly related to the force applied by the pilot. The magnitude of deflection is less significant, since it varies with airspeed.

The GAT-2 simulator has hydraulic control loading systems for developing simulated aerodynamic forces on elevators and ailerons. The amount of load is controlled by circuits that sense control deflection and dynamic air pressure to compute the load forces that would be felt by the pilot. A hydraulic servo loop in each system uses a valve, cylinder, and load cell to develop the computed force.

The following discussions describe the original force equations used in the GAT-2 simulator for control load computation, and describe modifications made to the simulator to represent the Cessna 421.

RUDDER FORCE LOADING.

The simulator rudder force equation is:

$$F_p = - K_p q(\delta_r^* + K_{tr}\,\delta_{ttr}^*) \pm F_{pf}$$

where: F_p = rudder pedal force, lb.

K_p = rudder pedal force coefficient, ft^2.

K_{tr} = rudder trim-tab ratio.

F_{pf} = rudder pedal friction force, lb.

q = aircraft dynamic pressure, lb/ft^2.

δ_r^* = nondimensional rudder deflection, $\pm$ 1.0 maximum. Equivalent to $\pm$ 25 deg. rudder, $\pm$ 2 inches pedal.

δ_{ttr}^* = nondimensional rudder trim tab deflection, $\pm$ 1.0 maximum.

The rudder pedals in the GAT-2 simulator do not have a hydraulic loading system, but are restrained by fixed springs. The resulting force gradient represents the loads that would occur at a typical dynamic pressure developed at low airspeed.

The original GAT-2 constants in the rudder force equation were:

$$K_p = 4.32 \text{ ft}^2$$

$$q = 22.5 \text{ lb/ft}^2, \text{ (a constant)}$$

$$K_{tr} = 0.775, \text{ (dimensionless ratio)}$$

$$F_{pf} = \pm 12.5 \text{ lb, (breakout force)}$$

Normal flying does not require much use of the rudder, so accurate representation of rudder forces over a wide range of airspeed conditions is not considered worthwhile. For this reason, the original GAT-2 had only a set of fixed springs, preloaded to represent friction breakout force. This lack of rudder use is particularly true for the type of flying intended for the Cessna 421 simulation.

Measurements of the actual Cessna rudder forces in flight verified that the simulator forces were in reasonable agreement with the actual aircraft at typical airspeeds, so no modifications were made to the original GAT-2 rudder loading system.

AILERON FORCE LOADING.

The simulator equation for aileron force at the control wheel is:

$$F_w = - K_w q(\delta_a^* + K_{ta} \delta_{tta}^*) \pm F_{wf}$$

where: F_w = aileron control wheel force, lb.

K_w = wheel force coefficient, ft^2.

K_{ta} = aileron trim-tab ratio.

F_{wf} = friction force at wheel, lb,

q = dynamic pressure, lb/ft^2.

δ_a^* = nondimensional aileron deflection, $\pm$ 1.0 maximum.
Equivalent to $\pm$ 40 deg. aileron, $\pm$ 110 deg. wheel.

δ_{tta}^* = nondimensional aileron trim-tab deflection, $\pm$ 1.0 maximum.

Flight measurements of the actual Cessna 421 aileron forces were compared with the GAT-2 aileron forces under similar conditions. These measurements showed that the simulator forces were in close agreement with those of the actual aircraft. Pilot opinions also verified that the forces were equivalent. As a result, no changes were made to the aileron control loading relations in the simulator.

The original GAT-2 constants in the aileron force equation were:

$$K_w = 0.64 \text{ ft}^2$$

$$K_{ta} = 0.045$$

$$F_{wf} = \pm 2 \text{ lb.}$$

ELEVATOR FORCE LOADING.

The simulator equation for elevator force at the control column is:

$$F_e = - K_e q(\delta_e^* + K_{te} \delta_{tte}^*) \pm F_{ef}$$

where:

F_e = elevator control column force, lb.

K_e = elevator force coefficient, ft^2.

K_{te} = elevator trim-tab ratio.

F_{ef} = elevator friction force, lb.

q = aircraft dynamic pressure, lb/ft^2.

δ_e^* = nondimensional elevator deflection, + 0.5, - 1.0, maximum.
Equivalent to: δ_e = + 15 deg., - 30 deg.
Control column: δ_s = + 2.68 in., - 5.38 in.

δ_{tte}^* = nondimensional elevator trim-tab deflection, - 0.43, + 1.0 maximum.

The original GAT-2 constants in the elevator force equation were:

$$K_e = 3.77 \text{ ft}^2.$$

$$K_{te} = 0.513, \text{ dimensionless ratio.}$$

$$F_{ef} = \pm 6 \text{ lb.}$$

Elevator forces are the most significant of the aircraft control loads, and therefore most important to represent correctly in the simulator. In addition to the typical elevator forces that result from maneuvers such as climbs, descents, and turns, a direct relationship exists between airspeed and elevator force. This is an indicator of the static stability of the aircraft. When loaded within proper limits of center of gravity, and with no change of trim control, a steady pushing force will be required to maintain an airspeed greater than an originally trimmed condition. Altitude will decrease in this case. Similarly, a steady pulling force will be required to maintain an airspeed below the trimmed speed, and altitude will increase. With release of either force, airspeed should return to the original trimmed condition.

Measurements of the actual control forces were made in flight tests of the Cessna 421, and in the GAT-2 simulator. Figure 7 illustrates the results of these tests, which show two significant differences between the aircraft and the simulator: the friction band was much larger in the GAT-2 than in the aircraft, and the slope of force versus airspeed was less in the GAT-2 than in the aircraft.

Modification of the control column bearing supports in the GAT-2 simulator reduced the mechanical friction to a level approximately half of that in the aircraft, as shown in the figure. This permitted adjustment of the friction terms in the control loading circuit to match the desired aircraft friction level.

Adjustment of the force slope terms in the loading circuit also permitted matching the slopes measured in the aircraft. As shown in the figure, the slope in the down elevator, or push, direction is steeper than for up elevator. Individual coefficients for push and pull forces in the loading circuit provide accurate matching of the two different slopes.

The values for the coefficients in the elevator control loading equation which have been selected to match the Cessna 421 characteristics are:

$K_e = 6.0\ ft^2$, for positive force (pull).

$K_e = 8.6\ ft^2$, for negative force (push).

$K_{te} = 0.513$, dimensionless.

$F_{ef} = \pm 1.0$ lb., friction force.

With these coefficients, the elevator control loads of the GAT-2 simulator are in good agreement with the actual Cessna 421 aircraft, as shown by force measurements and by pilot opinions.

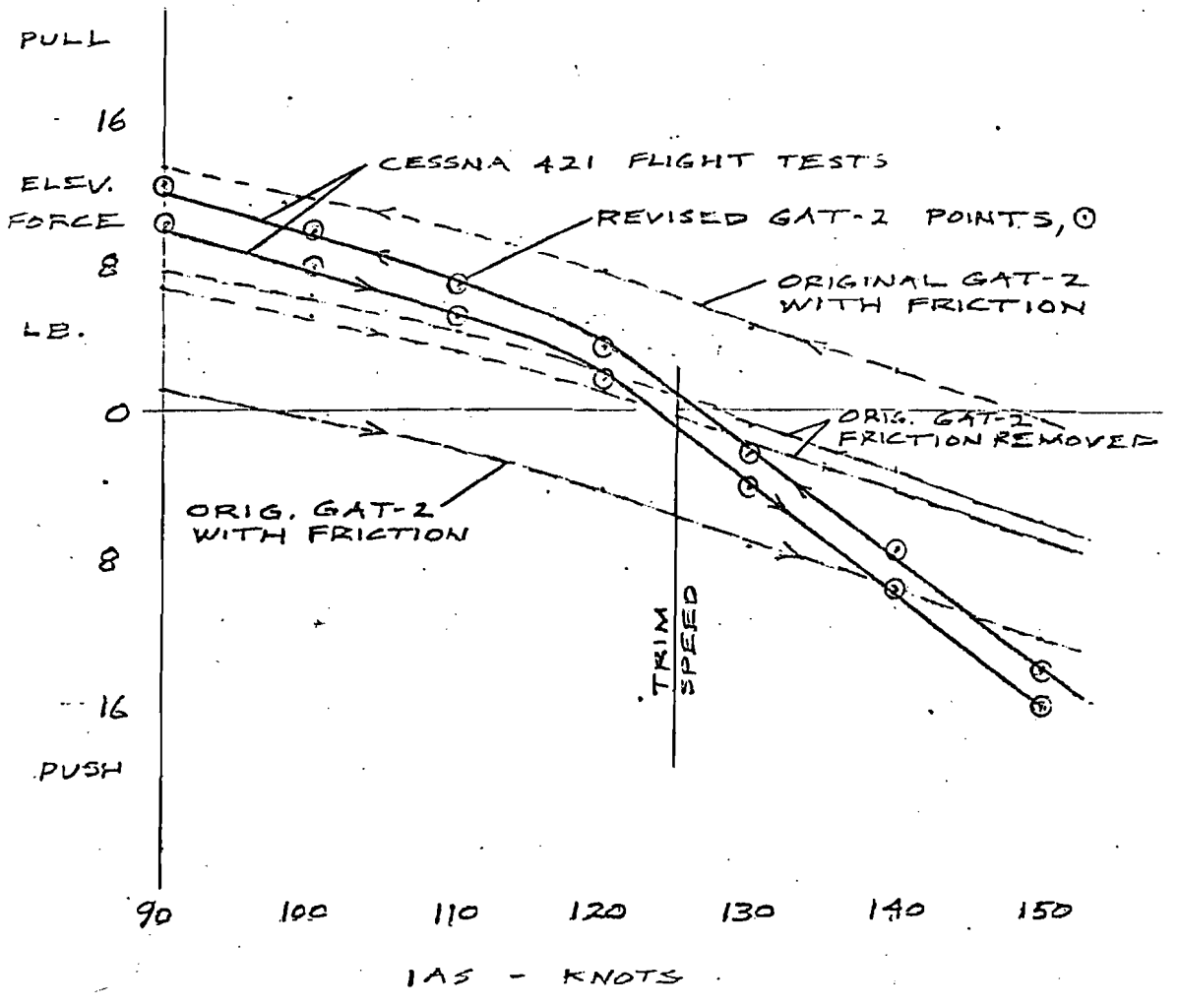

FIGURE 7. ELEVATOR FORCE VERSUS AIRSPEED

COMPARISON WITH FLIGHT DIRECTOR.

Originally, the GAT-2-B simulator was equipped with a Collins FD-109 Flight Director System. Conversion of the simulator to a representation of the Cessna 421 aircraft has required substitution of an autopilot for the flight director. The Collins AP-106 autopilot has been selected, as used in other Cessna 421 aircraft operated by the FAA.

In the flight director system, a computer determined the amount of turn, climb, or descent required to reach desired conditions of heading, course, or altitude. Guidance information displayed to the pilot on the Attitude Director Indicator (ADI) indicated the aircraft attitude necessary to meet these requirements. The pilot moved the elevators and ailerons to maneuver the aircraft until the attitude agreed with the guidance display.

A flight director control switch on the instrument panel permitted selection of the mode of operation, such as gyro, heading, navigation, approach, altitude-hold, and go-around. The gyro mode was equivalent to an off position, in which no guidance was provided by the flight director. A group of annunciator lights on the instrument panel indicated which modes were active.

The autopilot system is similar to the flight director, since it also includes a computer to determine the turn, climb, or descent required to reach desired conditions of heading, course, or altitude. The same ADI is used to provide guidance information. The principal difference between the autopilot and the flight director is the inclusion of servo actuators to move the elevators and ailerons as necessary to control the aircraft attitude.

An autopilot control head on the pedestal between the cockpit seats contains illuminated push-on, push-off selector switches for the various modes of operation. When a mode is selected, the corresponding pushbutton is lighted. Remote annunciator lights on the instrument panel, similar to those of the flight director, also indicate which modes are active. Details of the characteristics of the various modes are contained in appendix E.

The control head also contains a switch for engaging and disengaging the autopilot. When engaged, the servo actuators operate the controls to maneuver the aircraft in agreement with the guidance display. The pilot can monitor the display to verify proper autopilot operation. When disengaged, the autopilot reverts to the flight director configuration, in which the human pilot moves the controls manually to match the guidance display. Annunciator lights on the control head indicate whether the autopilot is engaged or disengaged.

A pitch-turn control is also mounted on the pedestal, which is used to change the aircraft attitude when the autopilot is in the basic attitude mode. Rotating knobs are provided for pitch and roll, which are spring-loaded to center detents. When a knob is rotated away from center, the attitude changes at a rate proportional to knob deflection. When the knob is returned to center, the attitude remains at the position existing at that time. If the pitch knob is rotated when a vertical guidance mode is active, the mode will be released and the autopilot will revert to a pitch hold condition. If the turn knob is rotated when a lateral guidance mode is active, the mode will be released (except in the cases of approach or go-around) and the autopilot will revert to a bank hold mode.

AUTOPILOT CONNECTIONS.

Figure 8 illustrates the input signals to the autopilot, and the outputs that are developed. Installation of the autopilot is similar to the flight director, but requires the addition of autopilot control heads and servo actuators for elevators and ailerons.

AIRCRAFT INPUTS. The fundamental task of the autopilot is to maintain commanded values of aircraft pitch and roll attitudes by manipulation of elevators and ailerons. The attitude commands may be made directly by the pilot, or computed to satisfy the requirements of the guidance modes. Measurements of the actual pitch and roll angles of the aircraft are basic reference information which must be sensed by the autopilot. In a real aircraft, these are normally synchro signals obtained from a vertical gyro. In the case of the flight simulator, computed values of roll angle and pitch angle are used to develop simulated synchro signals.

Additional signals of the aircraft's airspeed and altitude are applied as autopilot inputs for reference in modes where the autopilot is required to control either of these conditions.

NAVIGATION INPUTS. Signals of course deviation, glide-slope deviation, and distance measurement equipment (DME) are obtained from navigation radio receivers as inputs to the autopilot. These inputs are used with navigation and approach modes which require navigation signals from radio aids. The DME signal is used in conjunction with course deviation indicator (CDI) error to compute linear deviation magnitudes for CDI display.

PILOT INPUTS. The pilot can control various autopilot functions by a number of input signals: The control head provides the engage/disengage switch and mode selection signals from six push-on, push-off switches. Two pushbutton switches on the control wheel, or yoke, select the go-around mode and control wheel steering (CWS) condition. The pitch-turn control provides signals of pitch rate and roll rate as inputs to the autopilot in the attitude mode. An out-of-detent signal is also activated to cancel other modes when either the pitch or turn knob is rotated.

On the horizontal situation indicator (HSI), two knobs are available for pilot selection of heading or omni-bearing course. The signals provided to the autopilot by settings of these knobs are resolver error signals defining the difference between the current aircraft heading and the selected heading or course settings.

ANNUNCIATOR OUTPUTS. A group of annunciator outputs indicates the modes and conditions of the autopilot. Two lights on the control head indicate whether the autopilot is engaged or disengaged. Eight annunciator lights on the instrument panel show the operating modes and whether linear deviation is in effect. An annunciator on the ADI indicates when the go-around mode is active.

DISPLAY OUTPUTS. Pitch steering and roll steering output signals from the autopilot drive the command bars on the ADI, which define the required attitude of the aircraft when the autopilot is in a guidance mode. In the attitude mode, when the command bars are not used, an out-of-view signal from the autopilot drives the command bars to the top of the ADI, where they are not visible.

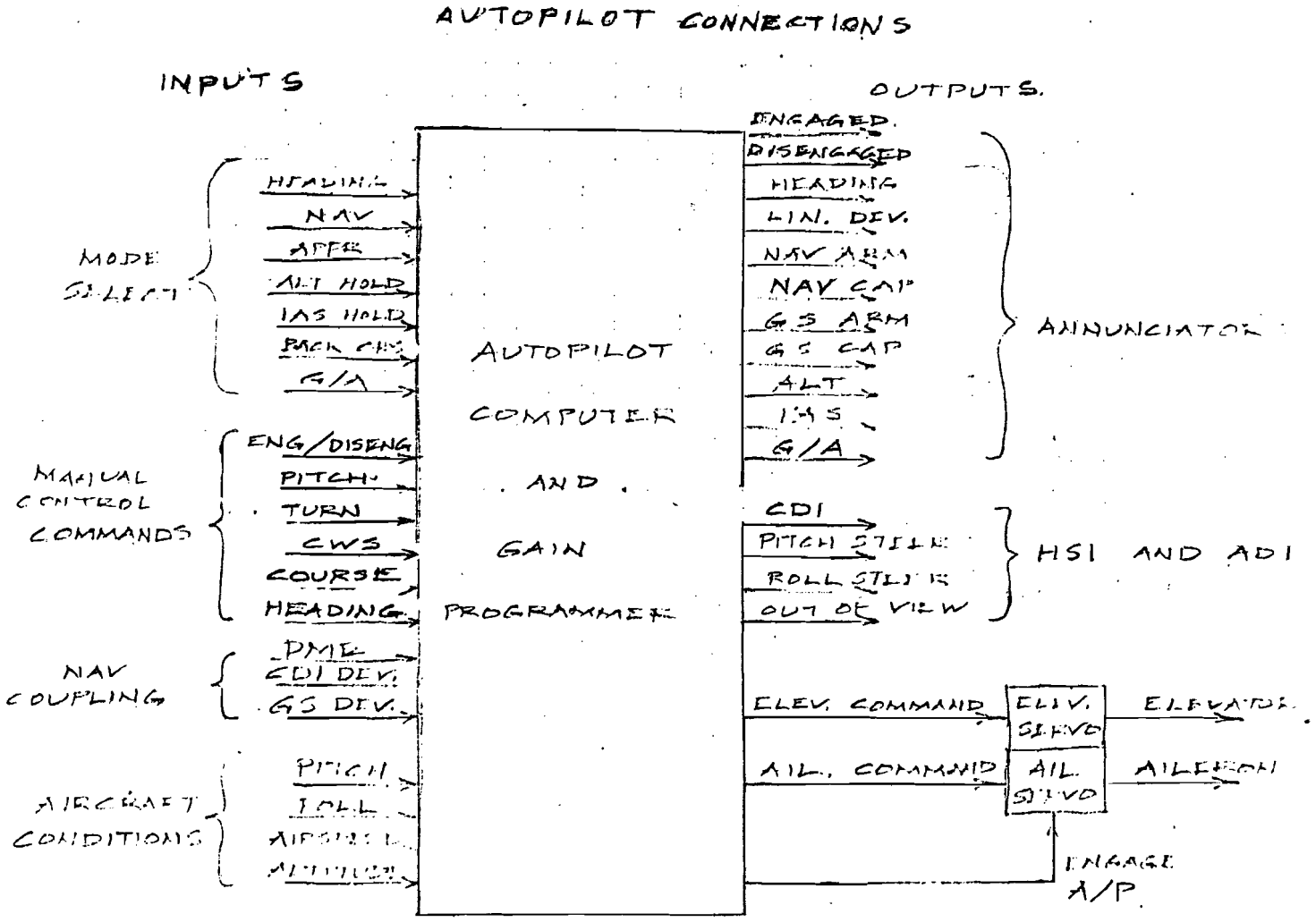

FIGURE 8. AUTOPILOT CONNECTIONS

A linear-deviation CDI signal, expressed in miles, is developed in the autopilot gain programmer by combining the angular CDI signal from a navigation receiver with the DME input signal. This signal becomes an autopilot output signal to the CDI needle on the HSI. When a localizer frequency is tuned, the signal reverts to the original angular CDI condition.

SERVO OUTPUTS. Signals of elevator and aileron position commands are supplied as outputs from the autopilot to the control servos. An autopilot engage signal output causes the servos to become active and move the control surfaces as necessary to match the position commands.

SERVO ACTUATION. In an actual aircraft, the autopilot installation employs electrically driven servo-actuators to move the elevator and aileron control cables. As the control surfaces move, the control wheels and columns in the cockpit also move.

For representation of the servo-actuator function in the flight simulator, a practical simulated servo approach has been taken which uses the hydraulic actuators of the control loading system to move the controls. As illustrated in figure 9, the simulated servo receives an autopilot command signal of desired control position and compares it with a feedback signal of actual control position. The difference between the two becomes a signal proportional to position error. A damping signal of control rate is also fed back for stabilization purposes.

The sum of the position error and rate signals is amplified in a servo amplifier to develop a force output signal, which is applied to the force summing point in the control loading circuit. The control loading hydraulic actuator will move the control wheel to minimize the force by matching the commanded position.

The servo force will match the magnitude of the simulated aerodynamic load, and will oppose any actual force applied to the control wheel by the human pilot. Limits are provided on the servo force signal, so that the human pilot can overpower the autopilot servo if desired.

When the autopilot is disengaged, the servo force signal is removed. The load system then reverts to its normal mode of operation, in which the human pilot moves the control wheel, and the hydraulic actuators provide resisting forces equivalent to the computed aerodynamic loads.

RESULTS OF MODIFICATIONS

In modifying the GAT-2 simulator to represent the Cessna 421 aircraft, emphasis has been placed on accuracy in aspects of the simulation that have the most significance in the intended studies. Since these studies will investigate influences on pilot workload, it is important that the pilot's perception of the response characteristics of the aircraft be realistic. Performance characteristics must also be correct, and navigational equipment must be accurate so that measurements of pilot performance will not be confused by equipment errors.

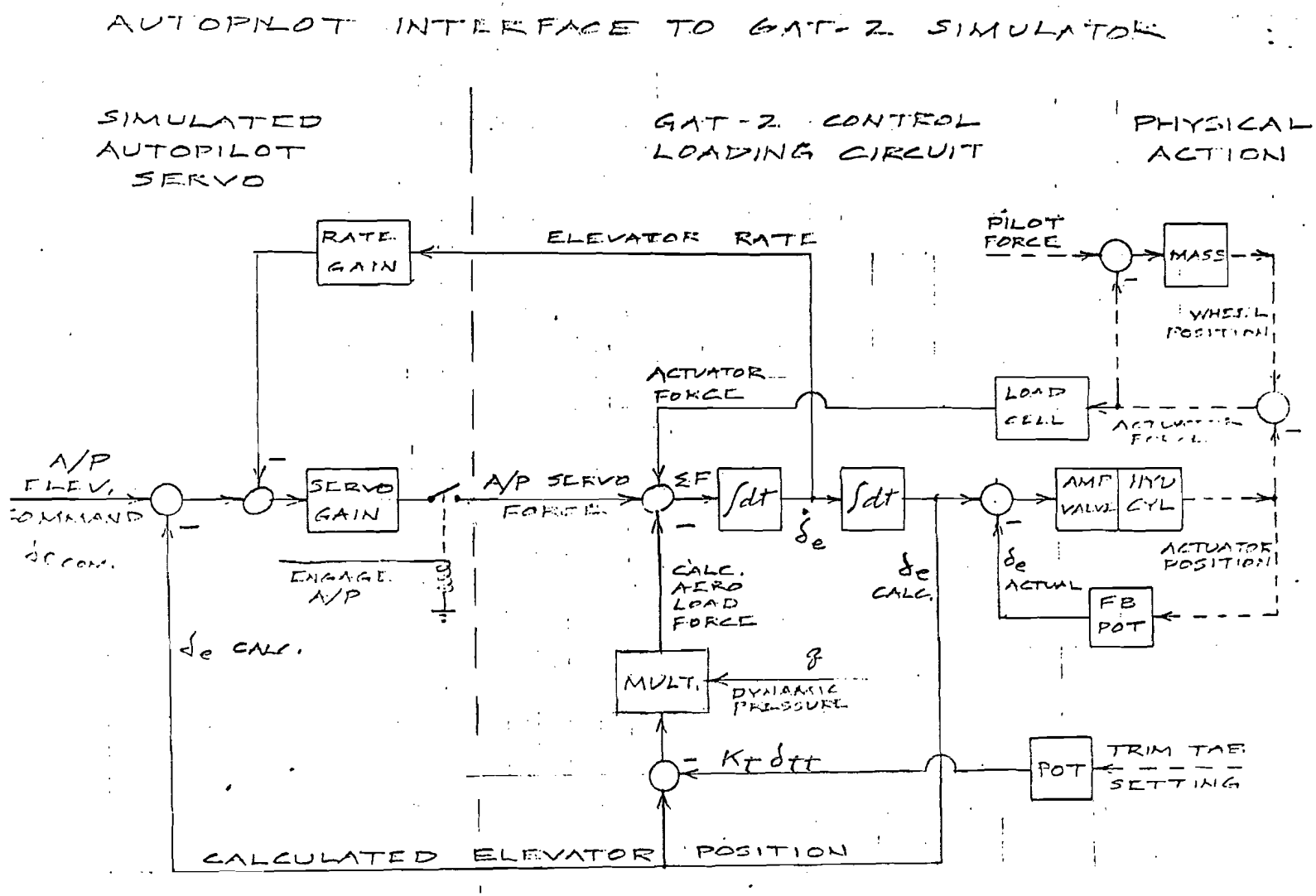

FIGURE 9. AUTOPILOT SERVO SIMULATION

To provide an accurate perception of response characteristics, a number of changes have been made that affect the pilot directly: Control force loading has been modified to match the Cessna 421. Engine power relations have been changed so that manifold pressure, propeller rpm, and fuel flow respond to throttle and propeller controls in the same manner as the aircraft. Stability characteristics have been changed, as necessary, where the computed derivatives are considerably different from the original GAT-2 values.

Performance characteristics have been matched to the Cessna 421 by modifying the relations among horsepower, thrust, and drag so that proper airspeeds are obtained for particular power settings. In combination with revised gross weight, these performance relations also produce proper climb and descent characteristics for departures, altitude changes, and landing approaches.

Navigational accuracy has been provided by careful adjustment of the coupling components that connect the navigation computations to autopilot equipment and to cockpit instrumentation. Adjustments have been made to the autopilot computer to match the aircraft characteristics so that accurate and responsive control of the aircraft is obtained during autopilot operation.

After completion of the modifications, a series of flight tests was performed on the simulator. These tests followed the form of flight test procedures for an actual aircraft. The results of the tests are reported separately in NAFEC Technical Letter Report NA-78-73-LR, prepared by Roman M. Spangler, dated June 1979, and entitled "Flight Characteristics of the NAFEC General Aviation Advanced Concepts Cockpit Evaluation Laboratory."

The results of the flight tests are summarized in that report by the following statements.

1. The simulator stall speeds were noted to be within 1 to 3 knots of the aircraft.

2. The simulator rate of climb performance was noted to duplicate the aircraft performance.

3. The single-engine rate of climb was precisely the same as the aircraft.

4. In penetrations from altitude, the rates of sink at penetration speeds were comparable to the aircraft.

5. Speed and power performance comparisons were conducted at 5,000, 10,000, and 15,000 feet altitude. The maximum variance was noted to be 3 percent or less.

6. Accelerations and decelerations of the GAT-2 simulator were compared with the Cessna 421, and found to be acceptable.

7. Turn rate versus bank angle and stick force versus bank angle showed an excellent comparison.

8. The general "feel" and "stick forces" that were measured also showed very good comparison with the aircraft.

9. The simulator longitudinal stability was also noted to be compatible.

10. The phugoid dynamics of the aircraft and the simulator were quite close.

11. Special investigations of the spiral divergence were also acceptable.

12. Evaluations of the GAT-2 avionics, navigation, and autopilot operation were quite comparable to the Cessna 421.

APPENDIX A

COMPUTATION OF AERODYNAMIC DERIVATIVES

This appendix describes details of methods used to determine values for coefficients used in the equations of motion. These methods are useful when values of the aerodynamic derivatives are not readily available from other sources, such as the aircraft manufacturer.

A three-view drawing of the desired aircraft is necessary for determining aircraft dimensions. An aircraft flight manual will provide additional information concerning weight, engine data, and performance relations.

The expressions for computing derivatives have been obtained from "Airplane Performance Stability and Control" by Perkins and Hage, and "Dynamics of Flight" by Bernard Etkin. These methods are intended for use in studying stability and control characteristics during aircraft design activities. They will provide coefficient values that are sufficiently accurate for normal simulation purposes.

When greater accuracy is needed for some particular purpose, determination of the derivatives that relate to that purpose may require additional data. In the case of the Cessna 421, drag derivatives have been determined by the methods described in the body of the report, in which drag, thrust, and power are matched to achieve the performance characteristics defined in the aircraft flight manual.

Values of the aerodynamic derivatives have been calculated by these methods for both the Cessna 310 and the Cessna 421 aircraft. The original GAT-2 values, which represented a Cessna 310, are also shown. Comparison of the calculated values with the original GAT-2 derivatives provides confidence in the validity of the method of computation.

Figure A-1, presents three-view drawings for both the Cessna 310 and Cessna 421 aircraft.

Dimensions obtained from the three-view drawings, and details of equations used for calculation of the derivatives are contained in tables A-1 through A-5.

FAA TECHNICAL CENTER
PROJECT USE ONLY
NOT FOR DISTRIBUTION

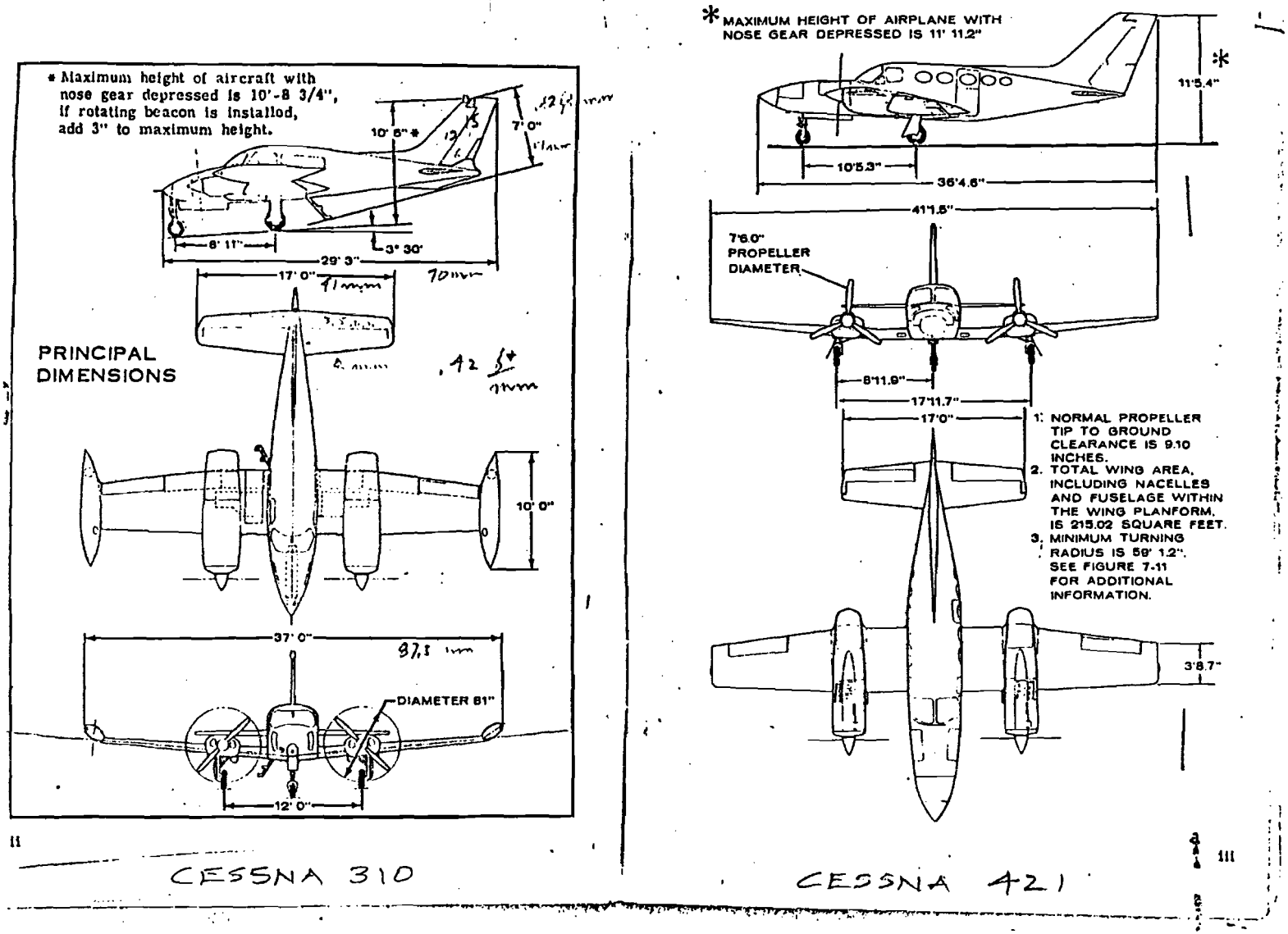

FIGURE A-1. THREE-VIEW DRAWINGS

TABLE A-1. AIRCRAFT DIMENSIONS

(Values obtained from three-view drawings)

	C-310	C-421	
A	7.66	8.28	Wing aspect ratio = $b/\bar{c}$
A_t	5.35	4.55	Tail aspect ratio = b_t/c_t
A_v	1.25	1.13	Vert. fin aspect ratio = b_v/c_v
b	37.00	41.83	Wing span, ft.
b_a	5.38	5.50	Aileron span, ft.
b_t	17.00	17.00	Tail span, ft.
b_v	6.30	7.48	Vert. fin span, ft.
$\bar{c}$	4.83	5.05	Wing mean aero. chord, ft.
c_a	1.18	1.32	Aileron chord, ft.
c_t	3.18	3.74	Tail chord, ft.
c_v	5.04	6.60	Vert. fin chord, ft.
c_w	4.41	4.40	Wing chord at aileron, ft.
l_t	15.30	17.60	Tail moment arm, ft.
l_v	15.30	17.60	Vert. fin moment arm, ft.
S	178.71	211.24	Wing area, ft^2 = $b\bar{c}$
S_e	24.70	20.30	Elevator area, ft^2
S_r	15.88	23.00	Rudder area, ft^2
S_t	54.06	63.58	Horiz. tail area, ft^2 = $b_t c_t$
S_v	31.75	49.37	Vert. fin area, ft^2 = $b_v c_v$
Γ	0.07	0.08	Dihedral angle, radians.
λ	0.67	0.67	Wing taper ratio.

TABLE A-2. EQUATIONS FOR DERIVATIVE COMPUTATION

C_{L_o}	$= -\alpha_{OL} C_{L_\alpha}$		
C_{L_α}	$= a_w = a_o / \left(1 + \frac{a_o}{\pi A} \right)$		p. 220 *
C_{D_o}	From performance data or airfoil data.		p. 484
$C_{D_{C_L^2}}$	$= \frac{1}{\pi A e}$, or from performance data.		p. 93
C_{D_β}	No expression available, use GAT-2 value.		
$C_{y_{\delta_r}}$	$= \frac{S_v}{S} \left(\frac{da_v}{d\delta_r} \right)$		(Etkin, p. 177, 180)
C_{y_β}	$= -2 a_v \left(1 - \frac{d\sigma}{d\beta} \right) \frac{S_v}{S}$, Approx. Fus.+ Tail.		(Etkin p. 168, 180)
$C_{\ell_{\delta_a}}$	$= -2\tau_a \left(C_{\ell_\delta} / \tau \right)$		p. 356, 358
C_{ℓ_β}	$= -\Gamma \left(C_{\ell_\psi} / \Gamma \right)$	Fig. 9-3,	p. 344, 345
C_{ℓ_p}	From plot.	Fig. 9-14,	p. 357
$C_{m_{ac}}$	From airfoil data.		p. 484
$C_{m_{\delta_e}}$	$= -a_t \bar{V} \left(da_t / d\delta_e \right)$	Eq. 5-73	p. 251
C_{m_q}	$= -1.1 \left(2 a_t \bar{V} l_t / \bar{c} \right)$ (Etkin p. 179)		p. 394
$C_{m_{\dot{\alpha}}}$	$= -2 a_t \bar{V} \left(l_t / \bar{c} \right) \left(d\epsilon / d\alpha \right)$		(Etkin p. 165, 179)
$C_{n_{\delta_r}}$	$= -a_v \frac{S_v}{S} \frac{l_v}{b} \left(\frac{da_v}{d\delta_r} \right)$		p. 324, 329
$C_{n_{\delta_a}}$	No expression available, use GAT-2 value.		
C_{n_β}	$= a_v \frac{S_v}{S} \frac{l_v}{b}$	Fig. 8-8	p. 324
$C_{n_{\dot{\beta}}}$	$= 2 a_v \frac{S_v}{S} \left(\frac{l_v}{b} \right)^2 \left(\frac{d\sigma}{d\beta} \right)$	Based on $C_{m_{\dot{\alpha}}}$ expression.	
C_{n_r}	$= -2 a_v \frac{S_v}{S} \left(\frac{l_v}{b} \right)^2 - \frac{C_D}{3}$		p.428

* Page and figure numbers refer to Perkins and Hage unless otherwise noted.

TABLE A-3. PARAMETERS USED IN DERIVATIVE COMPUTATIONS

α_{OL}	From airfoil data.	Angle of attack at zero lift.	p. 484 *
a_o	From airfoil data.	Section lift curve slope.	p. 484
a_w	$= \frac{a_o}{1 + a_o/\pi A}$	Wing lift curve slope.	p. 220
a_t	$= f\ (A_t)$	Tail lift curve slope.	Fig. 5-5, p. 221
a_v	$= f\ (1.55\ A_v)$	Vert. fin lift slope.	Fig. 8-8, p.324
e	From drag estimates.	Airplane efficiency factor.	p. 95
$d\epsilon/d\alpha$	$= 2\ a_w/\pi A$	Downwash derivative.	p. 222
$da_t/d\delta_e$	$= f\ (S_e/S_t)$	Tail lift derivative.	p. 250
$d\sigma/d\beta$	From GAT-2 value.	Sidewash factor.	(Etkin, p. 80, 82)
C_{ℓ_ψ}/Γ	$= f\ (A, \lambda)$	Dihedral influence.	Fig. 9-3, p. 345
C_{ℓ_δ}/τ	$= f\ (\frac{b_a}{b/2})$	Aileron influence.	Fig. 9-3, p. 356
τ_a	$= f\ (\frac{c_a}{c_w})$	Ail. effectiveness.	Fig. 9-15, p. 357
$\bar{V}$	$= S_t\ l_t\ /\ S\ \bar{c}$	Tail volume ratio.	p. 220
$da_v/d\delta_r$	$= f\ (S_r\ /\ S_v)$	Vertical fin lift derivative.	p. 250

* Page and figure numbers refer to Perkins and Hage unless otherwise noted.

TABLE A-4. PARAMETER VALUES

	C-310	C-421
α_{OL}	-0.021	-0.021
a_o	5.96	5.96
a_w	4.78	4.85
a_t	3.96	3.55
a_v	2.01	1.891
e	0.66	0.64
$d\epsilon / d\alpha$	0.397	0.373
$da_t / d\delta_e$	0.61	0.51
$da_v / d\delta_r$	0.65	0.62
$d\sigma / d\beta$	0.025	0.025
C_{ℓ_ψ} / Γ	0.75	0.75
C_{ℓ_δ} / τ	0.07	0.06
τ_a	0.59	0.58
$\bar{V}$	0.957	1.05

Dimensions in radians.

TABLE A-5. VALUES OF DERIVATIVES

	GAT-2	C-310	C-421
C_{L_o}	0.077	0.100	0.102
C_{L_α}	4.57	4.78	4.85
C_{D_o}	0.026		0.029
$C_{D_{C_L^2}}$	0.0625	0.0630	0.0597
C_{D_β}	0.1719		
$C_{y_{\delta_r}}$	0.1152	0.1155	0.1449
C_{y_β}	-0.6962	-0.6964	-0.8633
$C_{\ell_{\delta_a}}$	-0.0859	-0.0826	-0.0696
C_{ℓ_β}	-0.1014	-0.0525	-0.0600
C_{ℓ_p}	-0.5487	-0.520	-0.530
$C_{m_{ac}}$	-0.0144	-0.0150	-0.0150
$C_{m_{\delta_e}}$	-2.1360	-2.312	-1.901
C_{m_q}	-57.30	-26.41	-28.58
$C_{m_{\dot{\alpha}}}$	-57.30	-9.53	-9.69
$C_{n_{\delta_r}}$	-0.1152	-0.0960	-0.1153
$C_{n_{\delta_a}}$	0.0301		
C_{n_β}	0.1444	0.1477	0.1860
$C_{n_{\dot{\beta}}}$	0.0776	0.0031	0.0040
C_{n_r}	-0.1786	-0.11	-0.14

Dimensions are per radian.

APPENDIX B

MOMENT OF INERTIA APPROXIMATIONS

In addition to the coefficients and derivatives that define aircraft characteristics, values are also needed for the moments of inertia of the aircraft about the three axes of rotation. If values are not available from aircraft data or from the manufacturer, the methods described here may be used to estimate inertia values with sufficient accuracy for simulation purposes.

High accuracy is not necessary for moment of inertia values. Errors of 25 percent or more probably would not be detectable in simulator performance. In the system equations, moments of inertia determine the initial accelerations that occur in response to moment disturbances, such as those resulting from control deflections. After an acceleration has been initiated, angular rate rises quickly to an equilibrium level, and the acceleration decays to zero. The equilibrium rate is determined by a balance between the moment disturbance and the damping feedback term. This relationship is illustrated in figure B-1, which shows the time relationships of rolling rate and acceleration in response to aileron deflection. The responses in pitch and yaw are similar.

As shown in the figure, a step change of control deflection produces a moment which causes an initial angular acceleration. As angular rate increases in response to the acceleration, the damping feedback moment resulting from the rate will increase exponentially until it reaches an equilibrium with the control moment. The acceleration decays to zero as this equilibrium is approached. Calculation of the time involved in the exponential rise yields a characteristic time of approximately one quarter of a second at a typical flight condition. This indicates that angular rates are the significant responses to control deflections, while accelerations are temporary effects having only short durations. Inaccuracies of moment of inertia values will cause variations of the rise time that are not detectable unless the error is very large.

PROCEDURE FOR CALCULATING MOMENTS OF INERTIA.

The procedure outlined here provides a method for calculating values of moment of inertia about the three aircraft axes. The values obtained are only approximate, but are adequate for practical simulation purposes. The method requires the determination of weights and dimensions of various elements of the aircraft. The moment of inertia of each element is determined about each axis, using moment of inertia equations for typical types of bodies. The total inertia for each axis is the sum of the inertia values for the individual elements.

WEIGHT DETERMINATIONS.

Weight values for a particular aircraft are normally available from the flight manual. Engine weight may be found from Jane's "All the World's Aircraft," or approximated by multiplying the rated horsepower by a factor of 1.5 pounds per horsepower.

BLOCK DIAGRAM OF ROLL RESPONSE TO AILERON DEFLECTION:

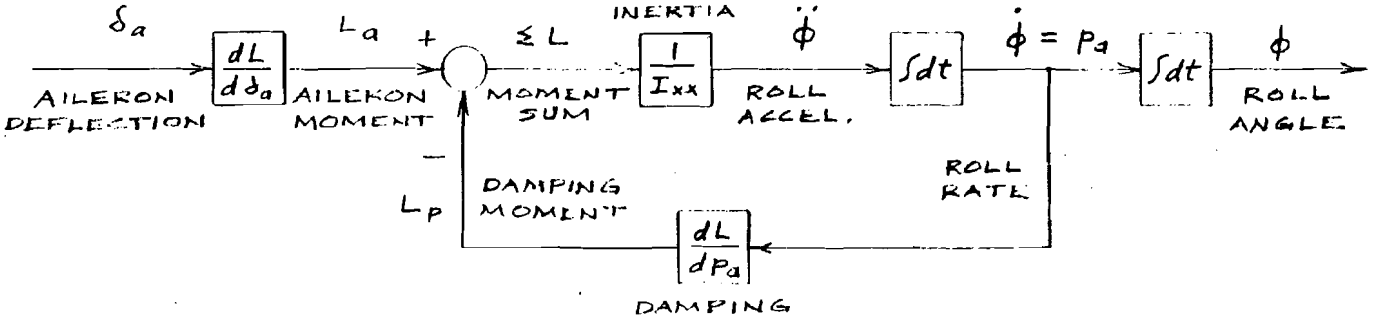

TIME RESPONSE:

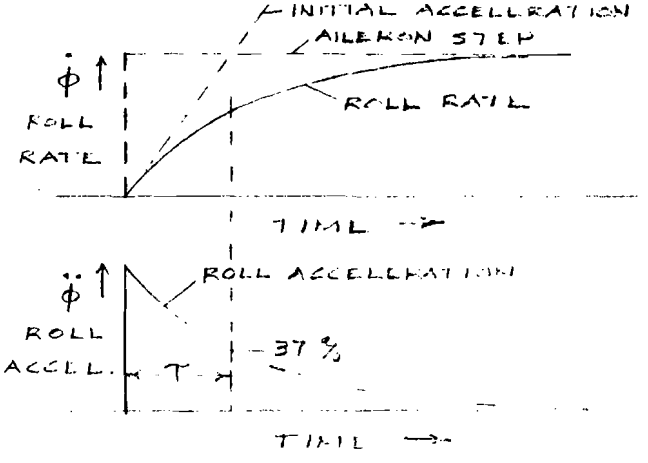

RESPONSE EQUATION:

$$\dot{\phi} = \left(\frac{G}{Ts+1}\right)\delta_a$$

STEADY-STATE GAIN:

$$G = \frac{dL/d\delta_a}{dL/dp_a} = \frac{2uC_{l_{\delta_a}}}{bC_{l_p}}$$

CHARACTERISTIC TIME:

$$T = \frac{I_{xx}}{dL/dp_a} \approx 0.25 \text{ SEC.}$$

$$dL/dp_a = qSb(b/2u)C_{l_p}$$

FIGURE B-1. TIME RESPONSE OF ANGULAR MOTION

The weights needed for moment of inertia calculations, and their values for the Cessna 421 aircraft are:

	Pounds (Cessna 421)
Maximum Gross Weight:	7450
Empty Weight:	4782
Engine Weight (2):	550 each = W_e
Fuel Weight:	
Main Tanks (2):	300 each = W_{tm}
Aux. Tanks (2):	210 each = W_{ta}
Nacelle Weight (2):	275 each
(Assume lumped weight of nacelle, landing gear, and associated equipment equals half the weight of an engine.)	
Structural Weight:	3132
(Subtract engine and nacelle weights from empty weight to get structural weight.)	
Wing Weight:	313 = W_w
(Assume wing weight equals one tenth of structural weight.)	
Fuselage Weight:	2819 = W_f
(Subtract wing weight from structural weight to get fuselage weight, including tail surfaces.)	
Payload Weight:	1648 = W_p
(Subtract empty weight and fuel from maximum gross weight to get payload weight.)	

DIMENSION DETERMINATIONS.

The distances from the aircraft center of gravity to the lumped masses, and the dimensions of various distributed masses, are determined from three-view drawings or data in the flight manual. The dimensions needed for moment of inertia calculations, and their values for the Cessna 421 aircraft are:

	Feet (Cessna 421)	
Fuselage Length:	33.8	= L_f
Fuselage Diameter:	5.0	= D_f
Cabin Length (Payload Space):	13.0	= L_c
Engine and Nacelle Lateral Dist.:	8.23	= R_e
Engine Forward Distance:	4.55	= L_e
Main Tank Lateral Distance:	5.0	= R_{tm}
Aux. Tank Lateral Distance:	12.0	= R_{ta}
Wing Span:	41.8	= b
Wing Taper Ratio:	0.667	= λ

EQUATIONS FOR MOMENT OF INERTIA.

Values of moment of inertia are computed by separating the aircraft into a number of individual elements on the basis of their shapes. The moment of inertia of each element is computed in accordance with the inertia equation for its particular shape.

Three equations are sufficient to compute moment of inertia values for all of the shapes into which the aircraft is divided in this simplified approach.

Lumped Mass:

In this case, the element is a concentrated mass at a distance, R, from the axis of rotation:

$$I = \frac{W R^2}{g}$$

where: I = moment of inertia, slug ft^2.

W = weight of element, lb.

R = distance from axis to element, ft.

g = 32.2 ft/sec^2, acceleration of gravity.

Uniformly Distributed Mass:

In this case, the moment of inertia is taken about an axis through the center of the element, perpendicular to the major dimension:

$$I = \frac{W L^2}{12 g}$$

where: L = major dimension, ft.

I, W, g are the same as above.

Cylinder:

In this case, the element is a uniform cylinder. The moment of inertia is taken about the longitudinal axis of the cylinder:

$$I = \frac{W D^2}{8 g}$$

where: D = diameter of the cylinder, ft.

I, W, g are the same as above.

ROLL MOMENT OF INERTIA.

For computing the roll moment of inertia, the engines, nacelles, and fuel tanks are taken as lumped elements at appropriate distances from the longitudinal axis. The fuselage, tail, and payload are combined as a cylinder about the axis. For simplicity, the effect of tail surfaces is assumed to compensate for the tapered shape of the fuselage. The combined element of fuselage and tail is then taken as a cylinder of constant diameter for computation of moment of inertia. The wing is taken as a distributed mass perpendicular to the axis. Since the wing is tapered, more accurate results have been found empirically by including the wing taper ratio as a factor in the expression for wing inertia.

ROLL INERTIA SUMMATION: Slug ft.^{2} (Cessna 421)

ENGINES:	$I_{ex} = 2 W_e R_e^2 / g$	=	2314
NACELLES:	$I_{nx} = 2(0.5 W_e) R_e^2 / g$	=	1157
MAIN TANKS:	$I_{tmx} = 2 W_{tm} R_{tm}^2 / g$	=	466
AUX. TANKS:	$I_{tax} = 2 W_{ta} R_{ta}^2 / g$	=	1878
WINGS:	$I_{wx} = \lambda W_w b^2 / 12 g$	=	943
FUS. & PAYLOAD:	$I_{fx} = (W_f + W_p) D_f^2 / 8 g$	=	434
ROLL MOMENT OF INERTIA SUM:	I_{xx}	=	7192

(Value obtained from Cessna Aircraft Co. : I_{xx} = 7119 to 7123)

PITCH MOMENT OF INERTIA.

In computing the pitch moment of inertia, the wings, nacelles, and fuel tanks are close to the lateral axis and provide negligible inertia.

The engines are taken as lumped elements at the appropriate distance forward of the lateral axis.

The fuselage and tail are considered as a uniformly distributed mass. Much of the fuselage weight, including seats, flooring, and other equipment is concentrated in the cabin area. It has been found empirically that a more accurate value is obtained by taking 75 percent of the fuselage weight distributed over the full length of the fuselage, and combining 25 percent of the fuselage weight with the payload in the cabin area.

PITCH INERTIA SUMMATION: Slug ft^2 (Cessna 421)

ENGINES:	$I_{ey} = 2 W_e L_e^2 / g$	=	707
FUSELAGE:	$I_{fy} = 0.75 W_f L_f^2 / 12 g$	=	6251
CABIN:	$I_{cy} = (0.25 W_f + W_p) L_c^2 / 12 g$	=	1029
PITCH MOMENT OF INERTIA SUM:	I_{yy}	=	7987

(Value obtained from Cessna Aircraft Co. : I_{yy} = 7659 to 8053)

YAW MOMENT OF INERTIA.

The yaw moment of inertia includes most of the terms used in the roll and pitch inertia computations. However, there are some redundant terms, since fuselage and engine elements appear in both the roll and pitch summations.

The cylindrical fuselage representation used for roll inertia does not apply to the yaw computation, and should be omitted.

For a twin engine aircraft, the lateral engine term of the roll computation adequately represents the engine influence in yaw. The forward engine term of the pitch computation should be omitted.

For a single engine aircraft, there will be no lateral lumped engine elements. The forward engine term will represent the engine on the nose of the aircraft, and should be included in the yaw computation.

The approximate moment of inertia in yaw may be computed by summing the roll and pitch inertia values and subtracting the individual terms that do not apply.

YAW INERTIA SUMMATION:			Slug ft^2 (Cessna 421)
ROLL INERTIA:	I_{xx}	=	7192
PITCH INERTIA:	I_{yy}	=	7987
FUSELAGE ROLL TERM:	$-I_{fx}$	=	-434
ENGINE PITCH TERM:	$-I_{ey}$	=	-707
YAW MOMENT OF INERTIA SUM:	I_{zz}	=	14038

(Value obtained from Cessna Aircraft Co. : I_{zz} = 13110 to 13508)

APPENDIX C

MODIFICATION OF GAT-2 COMPUTER FOR REVISED COEFFICIENTS

The aerodynamic equations of motion are mechanized in the GAT-2 simulator by analog computer circuits. Coefficients in the equations are represented by the gain magnitudes of individual amplifiers in the circuits. These gain values are determined by the input and feedback resistors at each amplifier. To change coefficients, resistors of different magnitudes are substituted for the original resistors in the circuits.

Calculations of the appropriate gain and resistor values are based on the desired coefficient values and the scale factors of the associated variables. Each variable in the equations is represented by a voltage in the computer. The magnitude of each variable is related to the corresponding voltage by a scale factor, which is selected to match the variable to the maximum voltage range of the computer.

Figure C-1 illustrates the gain relationship of a typical analog amplifier, and the relations among gains, coefficients, and scale factors. Each analog voltage equals the magnitude of a variable divided by the corresponding scale factor. The gain of an analog amplifier is the ratio of the output voltage to the input voltage, which is determined by the ratio of the feedback resistor to the input resistor. The gain required to represent a specified coefficient is calculated by multiplying the coefficient by the ratio of input to output scale factors. From the calculated gain, the necessary resistor values can be determined.

As illustrated in figure C-2, several input variables can be added algebraically to influence one output variable. In this case, an individual gain value is determined for each input by the ratio of the feedback resistor to the corresponding input resistor.

Figures C-3 and C-4 show representative cases which illustrate the procedures used to modify the analog computer gain relations. These cases are typical of all of the changes that have been made to modify the GAT-2 simulator to represent the Cessna 421 aircraft.

The time required to remove and install new resistors in the necessary locations is less than one day, which is short in comparison with the weeks involved in determining the values of coefficients for a particular type of aircraft. If frequent interchanges among types of aircraft are desired after all coefficients are known, more rapid changing of resistor values could be achieved by using potentiometers in place of fixed resistors at necessary locations.

REPRESENTATION OF COEFFICIENTS ON AN ANALOG COMPUTER:

BASIC EQUATION: $y = C\,x$

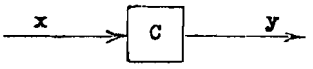

ANALOG AMPLIFIER RELATIONS:

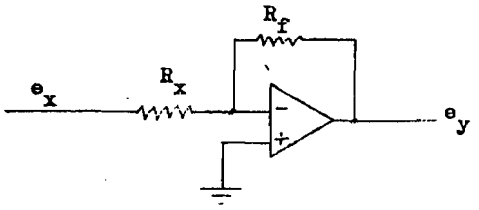

$$e_y = -G\,e_x \text{ , volts.} \qquad G = \frac{R_f}{R_x}$$

$$\frac{y}{u_y} = \left(-\frac{R_f}{R_x}\right)\frac{x}{u_x} \text{ , volts.} \qquad G = \frac{u_x}{u_y}C$$

$$y = \left(-\frac{R_f}{R_x}\frac{u_y}{u_x}\right)x \qquad C = \frac{R_f}{R_x}\frac{u_y}{u_x}$$

$$y = -C\,x$$

where:

- x = input variable, with dimensions.
- y = output variable, with dimensions.
- u_x = input scale units per volt.
- u_y = output scale units per volt.
- $e_x = \frac{x}{u_x}$, input voltage.
- $e_y = \frac{y}{u_y}$, output voltage.
- R_x = input resistor value, ohms.
- R_f = feedback resistor value, ohms.
- C = coefficient relating y to x, with dimensions.
- G = amplifier gain, dimensionless.

FIGURE C-1. ANALOG AMPLIFIER RELATIONS

SUMMATION OF TERMS ON AN ANALOG COMPUTER.

BASIC EQUATION: $$y = C_1 x_1 + C_2 x_2 + C_3 x_3$$

ANALOG AMPLIFIER REPRESENTATION:

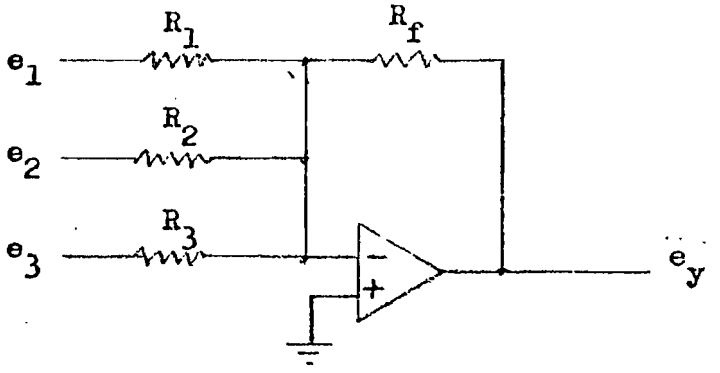

$$e_y = -C_1 e_1 - C_2 e_2 - C_3 e_3$$

$$e_y = -\frac{R_f}{R_1} e_1 - \frac{R_f}{R_2} e_2 - \frac{R_f}{R_3} e_3$$

$$\frac{y}{u_y} = -\frac{R_f}{R_1}\frac{x_1}{u_1} - \frac{R_f}{R_2}\frac{x_2}{u_2} - \frac{R_f}{R_3}\frac{x_3}{u_3}$$

$$y = -\left(\frac{R_f}{R_1}\frac{u_y}{u_1}\right) x_1 - \left(\frac{R_f}{R_2}\frac{u_y}{u_2}\right) x_2 - \left(\frac{R_f}{R_3}\frac{u_y}{u_3}\right) x_3$$

$$y = -C_1 x_1 - C_2 x_2 - C_3 x_3$$

FIGURE C-2. ANALOG SUMMATION OF MULTIPLE INPUTS

ORIGINAL ENGINE SPEED COMPUTATION (IN GOVERNING RANGE) :

$$N = 1650 + 950\,\delta^*_{pc} \quad , \text{ RPM}$$

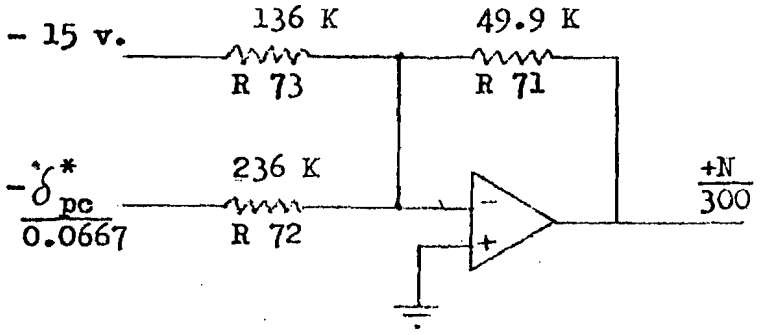

$$\frac{N}{300} = -\frac{49.9}{136}(-15) - \frac{49.9}{236}\left(\frac{-\delta^*_{pc}}{0.0667}\right) \quad , \text{ volts}$$

REVISED PROPELLER SPEED COMPUTATION (IN GOVERNING RANGE) :

$$N_p = 1300 + 975\,\delta^*_{pc} \quad , \text{ RPM}$$

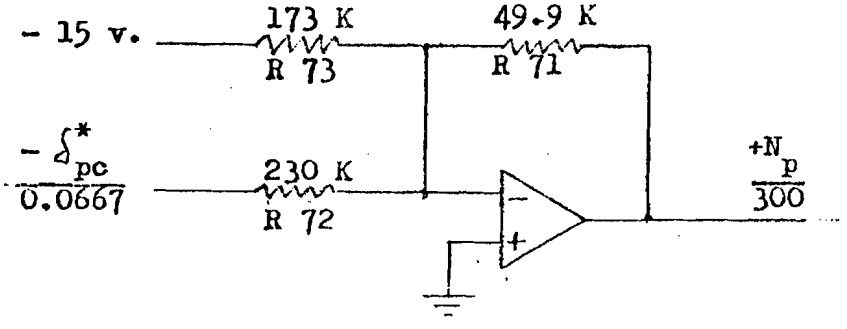

$$\frac{N_p}{300} = -\frac{49.9}{173}(-15) - \frac{49.9}{230}\left(\frac{-\delta^*_{pc}}{0.0667}\right) \quad , \text{ volts}$$

FIGURE C-3. ENGINE SPEED REVISION

ORIGINAL MANIFOLD PRESSURE COMPUTATION:

$$MAP = 29.92 - 0.00076\,N - 0.0009\,h - 0.0165\,(1 - \delta^*_{th})^2\,N \quad \text{in. Hg.}$$

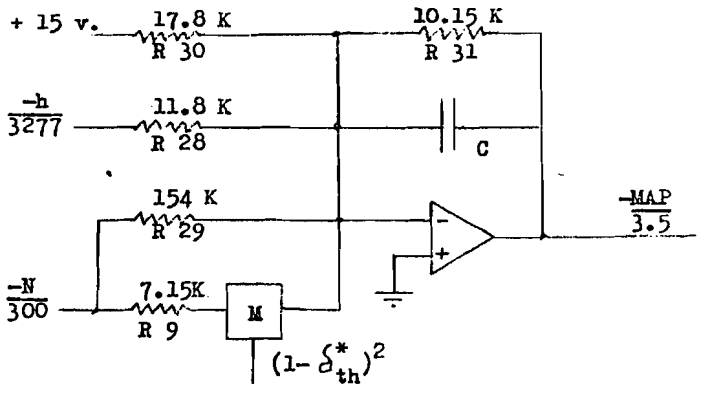

$$-\frac{MAP}{3.5} = -\frac{10.15}{17.8}(15) - \frac{10.15}{154}\left(\frac{-N}{300}\right) - \frac{10.15}{11.8}\left(\frac{-h}{3277}\right) - \frac{10.15}{7.15}(1-\delta^*_{th})^2\left(\frac{-N}{300}\right) \text{ volts}$$

REVISED MANIFOLD PRESSURE COMPUTATION:

$$MAP = 29.92 + 0.0048\,N_p - 0.025\,(1 - \delta^*_{th})^2\,N_p \quad \text{in. Hg.}$$

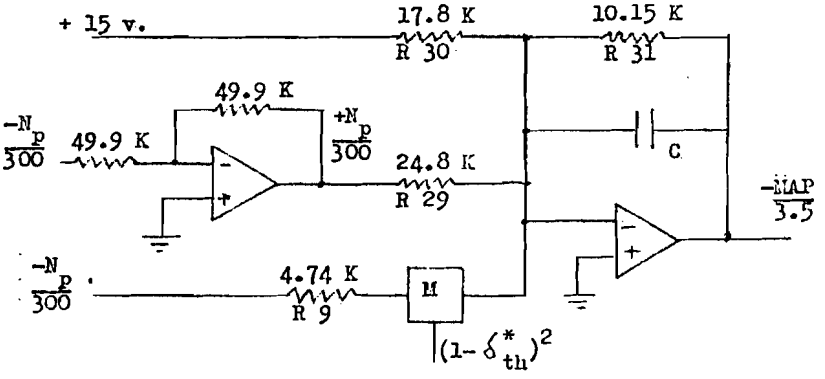

$$-\frac{MAP}{3.5} = -\frac{10.15}{17.8}(15) - \frac{10.15}{24.8}\left(\frac{N_p}{300}\right) - \frac{10.15}{4.74}(1-\delta^*_{th})^2\left(\frac{-N_p}{300}\right) \text{ volts}$$

FIGURE C-4. MANIFOLD PRESSURE REVISION

APPENDIX D

PHUGOID RESPONSE RELATIONS

The phugoid response of an aircraft results from an interchange of potential and kinetic energy between the vertical and forward degrees of freedom. Although the pitch angle, θ, and the flight path angle, γ, vary considerably during this oscillation, the angle of attack, α, has only a small variation. This results from the small requirement for variation of the lift coefficient, C_L, as the airspeed varies a small percentage about the nominal value.

To make a simplified determination of the aircraft characteristics that influence phugoid response, a closed-loop representation of the vertical and forward equations alone can be made, while ignoring the pitch equation and assuming the lift coefficient to be constant. This approach provides an approximate solution which illustrates the influences that determine phugoid period and damping characteristics.

For this analysis, translation equations 4 and 6 from table 1 can be expressed in linearized form to develop the loop relations for forward and vertical motions. Thrust, weight, C_L, and C_D are constants. Roll angle, ϕ, is zero, and $\sin\gamma = \gamma$ in radians. The variables shown in these expressions represent perturbations about nominal values of an initially equilibrium condition.

EQ. 4 : FORWARD ACCELERATION, LINEARIZED:

$$d\dot{u} = -\left(\frac{g}{W} S C_D\right)dq - (g)d\gamma$$

EQ. 6 : VERTICAL ACCELERATION, LINEARIZED:

$$d\dot{w} = -\left(\frac{g}{W} S C_L\right)dq$$

From the relation $q = \rho u^2/2$, the derivative is:

$$dq = (u\rho)du$$

From the relation $\dot{\gamma} = -\dot{w}/u$, with zero as the nominal value of $\dot{w}$, the derivative is:

$$d\dot{\gamma} = -\left(\frac{1}{u}\right)d\dot{w}$$

The linearized block diagram that results from these expressions is shown in figure D-1. This diagram may be reduced to the standard form of a quadratic dynamic loop as shown in figure D-2. From this loop, the resulting response equation is:

$$\frac{y}{x} = \frac{1}{s^2 + G_2 s + G_1}$$

A typical expression for the response of a quadratic dynamic loop is:

$$\frac{y}{x} = \frac{1}{s^2 + 2\zeta\omega_n s + \omega_n^2}$$

where: ω_n = natural frequency, radians/sec.

ζ = damping ratio.

s = Laplace operator.

From these two response equations, the gain relations are:

$$G_1 = \omega_n^2$$

$$G_2 = 2\zeta\omega_n$$

Expressions for G_1 and G_2 may be obtained from the block diagram, using the following relation for aircraft weight equal to lift:

$$W = \rho u^2 S C_L / 2$$

Then G_1 and G_2 become:

$$G_1 = \left(\frac{1}{u}\right)(g)(u\rho)\left(\frac{2gSC_L}{\rho u^2 S C_L}\right)$$

$$G_1 = 2g^2 / u^2$$

$$G_2 = (u\rho)\left(\frac{2gSC_D}{\rho u^2 S C_L}\right)$$

$$G_2 = \frac{2g}{u}(C_D / C_L)$$

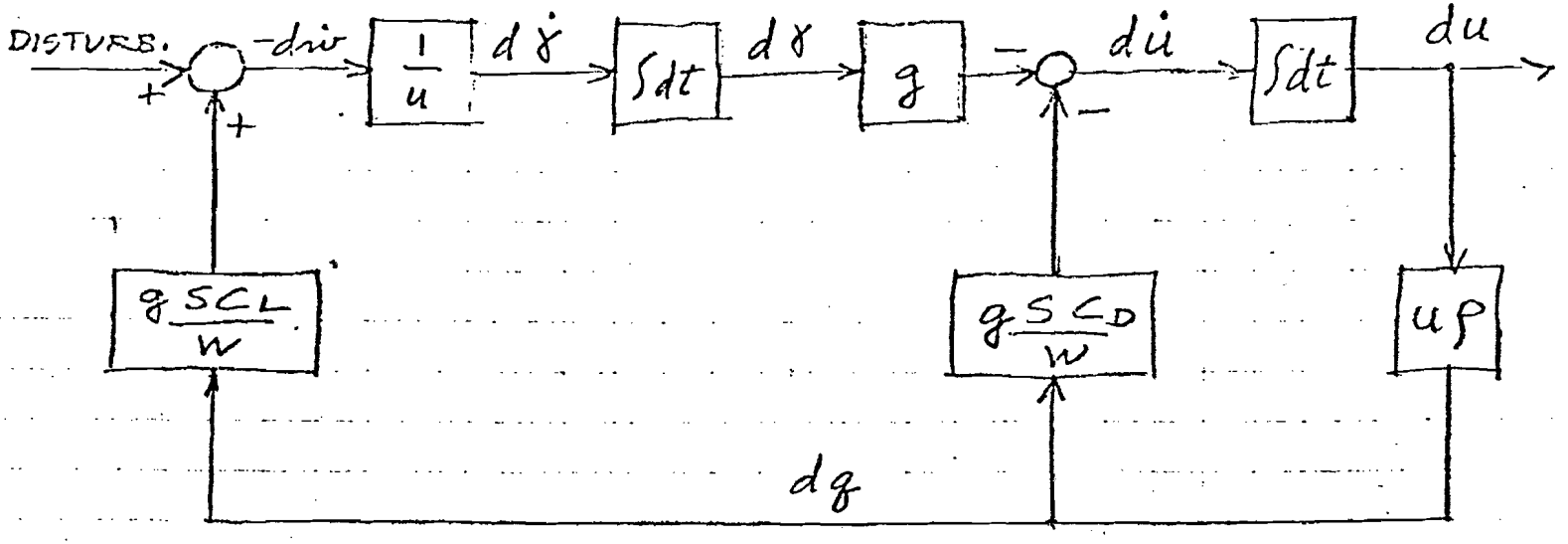

FIGURE D-1. BLOCK DIAGRAM OF LINEARIZED VERTICAL AND FORWARD EQUATIONS

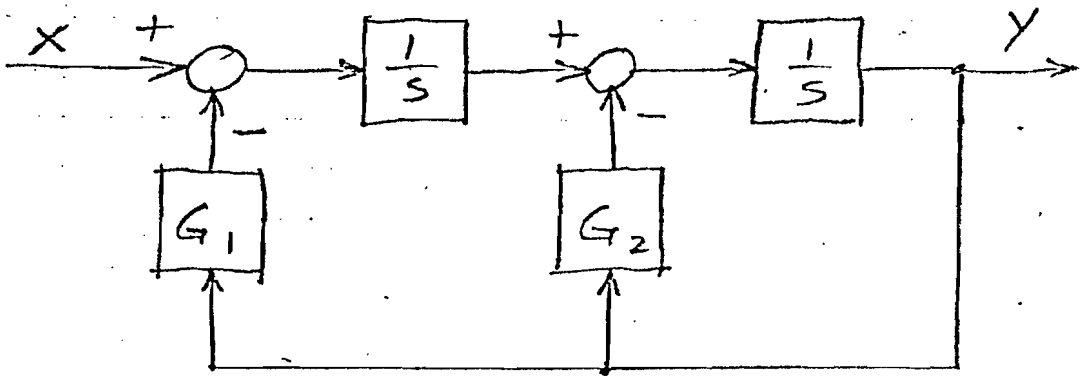

X = DISTURBANCE
Y = RESPONSE
1/S = TIME INTEGRATION
G_1 = LOOP GAIN
G_2 = DAMPING GAIN

FIGURE D-2. QUADRATIC DYNAMIC LOOP

The solutions for natural frequency, period, and damping for the phugoid oscillation are then:

PHUGOID NATURAL FREQUENCY:

$$\omega_n = \sqrt{\frac{2g^2}{u^2}} = \frac{g\sqrt{2}}{u} \quad \text{radians/sec}$$

PHUGOID PERIOD:

$$P = \frac{2\pi}{\omega_n} = \frac{\pi u \sqrt{2}}{g} = 0.138\,u \quad \text{seconds}$$

DAMPING RATIO:

$$\zeta = \frac{G_2}{2\omega_n} = \left(\frac{2gC_D}{uC_L}\right)\left(\frac{u}{2g\sqrt{2}}\right) = \frac{C_D}{C_L\sqrt{2}}$$

DECAY RATE OF PHUGOID AMPLITUDE:

$$\frac{A_2}{A_1} = e^{-\zeta\omega_n t}$$

For a time equal to the phugoid period, this becomes:

$$\frac{A_2}{A_1} = e^{-\pi\sqrt{2}\,C_D/C_L}$$

This gives the amplitude ratio between successive peaks, one cycle apart.

These solutions show that the period of phugoid oscillation for any aircraft depends only upon the airspeed and is not related to size or weight. Once a phugoid oscillation has been initiated, the damping, or rate of decay, of the oscillation will depend upon the lift to drag ratio of the aircraft. The cleaner the aircraft, the longer the oscillations will persist.

A more complete computation, including the pitch degree of freedom, provides a quartic solution which defines the short period response to disturbances as well as the phugoid oscillation. The result is similar, with the phugoid period dependent upon airspeed, but the magnitude of the period is somewhat longer:

PHUGOID PERIOD, MORE ACCURATELY:

$$P = 0.18\,u, \quad \text{seconds.}$$

Flight tests were run on both the Cessna 421 aircraft and the GAT-2 simulator at an initial altitude of 4200 feet, and an initial indicated airspeed of 122 knots. The true airspeed of this condition is 219 ft/sec, which results in a predicted phugoid period of 39.4 seconds.

Using the expression for aircraft weight equal to lift, $W=qSC_L$, results in a value of 0.7 for C_L. The expression for drag in table 6 provides a drag coefficient relation which results in a value of $C_D = 0.058$ and an L/D of 12. The predicted ratio of phugoid amplitude that results from these values is 0.69 per cycle.

The actual results of the flight tests, illustrated in figure D-3, are in good agreement with the computations. Both the Cessna 421 and the GAT-2 show phugoid periods of approximately 40 seconds and amplitude ratios of approximately 66 percent per cycle, which verifies that the simulator equations properly represent the Cessna 421 response.

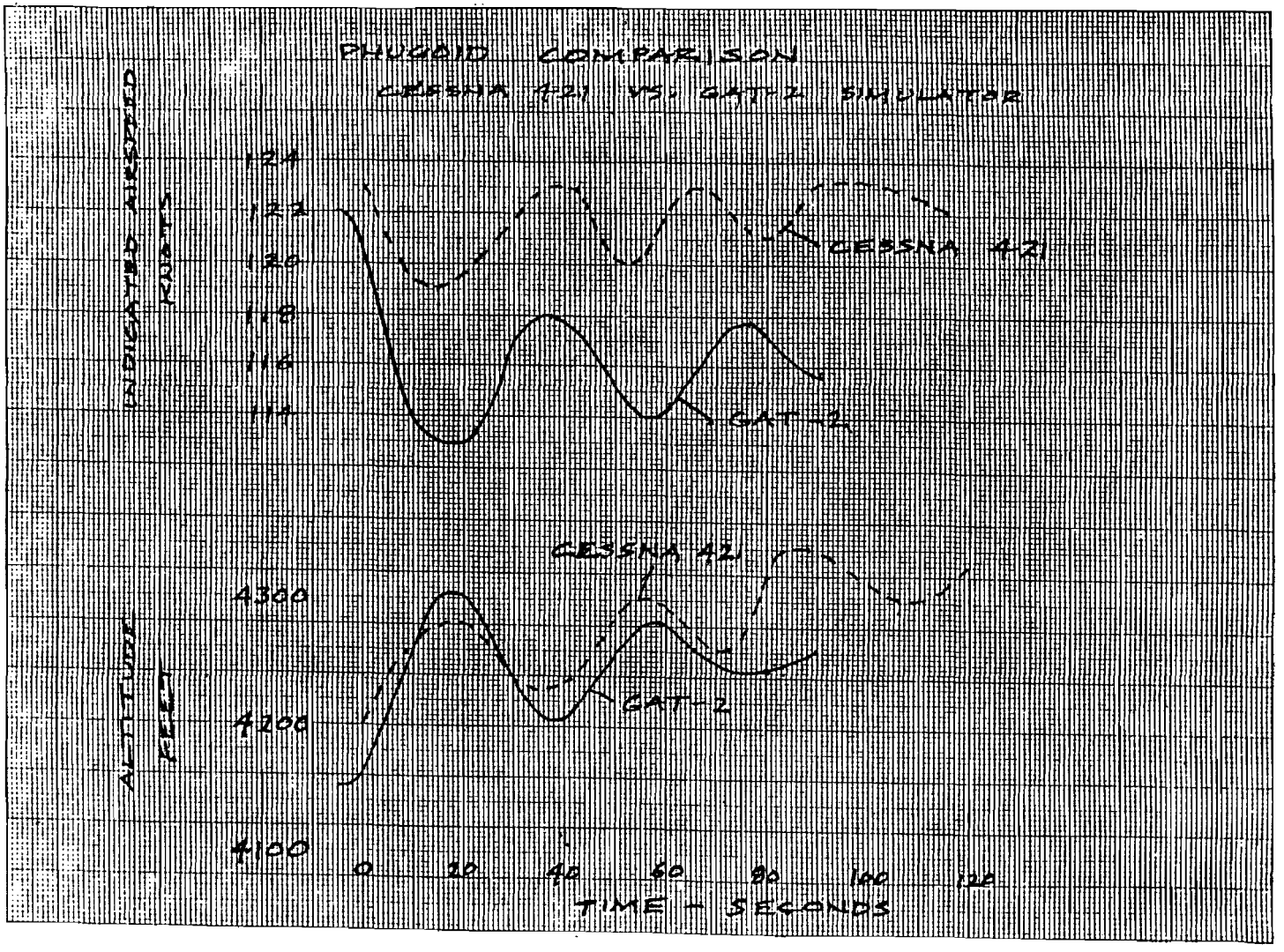

FIGURE D-3. PHUGOID RESPONSE OF GAT-2 AND CESSNA 421

APPENDIX E

AUTOPILOT MODES OF OPERATION

In the AP-106 autopilot, several modes of operation are available to the pilot, which can be selected by depressing the push-on, push-off switches on the autopilot control head. When a mode is on, the corresponding switch is lighted, and the appropriate annunciator is also lighted on the instrument panel. The flight director guide bars are in view when any guidance mode is on. If the autopilot is engaged, it will maneuver the aircraft to match the guide bars. If disengaged, the pilot must fly the aircraft manually to match the guide bars.

The guidance modes include the vertical modes of altitude hold and indicated airspeed hold, and the lateral modes of heading, navigation, approach, and back course. In addition, a go-around mode is available, which is selected by depressing a button on either control wheel. An annunciator light on the Attitude Director Indicator (ADI) indicates when the go-around mode is on.

ATTITUDE MODE.

When no guidance mode has been selected, and the autopilot is engaged, the attitude mode is in operation. This is similar to the gyro mode of the flight director, in which no guidance mode has been selected and no annunciator is lighted. The guide bars are out of sight and the autopilot acts to maintain the pitch and roll attitudes that existed when the engage switch was energized. These attitudes can be changed by manually rotating the knobs on the pitch-turn control, or by using the control wheel steering (CWS) feature. This is accomplished by depressing the CWS button on either control wheel, which disengages the autopilot servos. The pilot can then manually fly the aircraft to a new attitude. When the CWS button is released, the autopilot will maintain the attitude which exists at that time. No mode annunciator is lighted in the attitude mode.

ALTITUDE HOLD MODE.

In the altitude hold mode, the autopilot controls the elevators to maintain altitude at a desired level. Airspeed is varied by manual adjustment of engine power.

The altitude hold mode acts to maintain the barometric altitude that existed when that mode switch was depressed. The guide bars are in view and move vertically to indicate the pitch attitude required to reach and maintain the set altitude. When the autopilot is engaged, the servo moves the elevators as necessary to meet the required pitch attitude. When disengaged, the pilot moves the elevators manually to match the pitch attitude to the guide bars.

To change the selected altitude setting, the altitude hold mode must be disengaged by depressing the mode switch or CWS button. The pilot then flies the aircraft to the new desired altitude, and the mode switch is depressed again to engage the altitude hold mode.

This mode may be engaged at the same time as any of the lateral modes. Engagement of indicated airspeed (IAS)-hold mode or capture of a glide-slope will cause the altitude hold mode to disengage.

INDICATED AIRSPEED-HOLD MODE.

In the IAS-hold mode, the autopilot controls the elevators to hold indicated airspeed at a desired level, while climb or descent rate is controlled by manual adjustment of engine power.

The IAS-hold mode acts to maintain indicated airspeed at the level which existed when that mode switch was depressed. The guide bars are in view and move vertically to indicate the pitch attitude required to reach and maintain the set airspeed. When the autopilot is engaged, the servo moves the elevators as necessary to meet the required pitch attitude. When disengaged, the human pilot moves the elevators manually to match the pitch attitude to the guide bars.

To change the selected airspeed setting, the IAS-hold mode must be disengaged by depressing the mode switch or the CWS button. The pilot then flies the aircraft manually to the new desired airspeed, and the mode switch is depressed again to engage the IAS-hold mode.

This mode may be engaged at the same time as any of the lateral modes. Engagement of altitude-hold mode, or glide-slope capture, will cause this mode to disengage.

HEADING MODE.

When the heading (HDG) mode is selected, the autopilot controls the ailerons to turn the aircraft until the heading of the aircraft matches a reference heading selected by the pilot.

The heading reference is selected by rotation of a knob on the horizontal situation indicator (HSI), which moves an indicator to the desired heading on the compass card. An error signal of the difference between actual aircraft heading and selected heading is provided as an input to the autopilot. When the heading mode switch is engaged, the guide bars are in view and rotate left or right to indicate the roll attitude required to reach and maintain the desired heading. When the autopilot is engaged, the servo moves the ailerons as necessary to meet the required roll attitude, which is limited to a maximum bank angle of 25 degrees. When disengaged, the pilot moves the ailerons manually to match the roll attitude to the guide bars.

NAVIGATION MODE.

In the navigation (NAV) mode, the autopilot controls the aircraft to follow a selected VOR radial or localizer bearing. Since this mode uses signals from a navigation receiver as input information, a correct VOR or localizer frequency must be tuned. The desired VOR radial is selected by the course knob on the HSI. Inputs to the autopilot for the NAV mode are CDI error from the navigation receiver and course error from the HSI.

When the NAV mode is selected, if the aircraft is more than 10 miles from the selected radial, the CDI needle will have full deflection. The "V/L ARM," "HDG," and "LIN DEV" annunciators will be lighted, signifying that the desired radial has not been captured, that heading mode is active, and that deflections on the CDI needle represent linear deviations in miles.

The heading knob on the HSI can be adjusted to select an aircraft heading that intersects the desired radial at an angle of 90 degrees or less. As the aircraft follows this heading and approaches the desired radial, CDI deflection will decrease. When the deflection has reduced to a certain level, capture of the radial occurs. The "V/L CAP" annunciator is lighted, and the "V/L ARM" and "HDG" annunciators are turned off. Autopilot guidance will turn the aircraft to alignment with the selected radial, and will track the radial to keep the CDI centered.

APPROACH MODE.

The approach (APPR) mode provides lateral guidance along a localizer bearing, and vertical guidance along a glide slope, for an ILS landing approach. Since this mode uses signals from navigation receivers as input information, the proper frequency for the desired ILS approach must be tuned. The appropriate localizer bearing must also be set by the course selector knob on the HSI. Inputs to the autopilot for the approach mode are CDI error and glide-slope error from the corresponding receivers, and course error from the HSI.

If the aircraft is more than 2.5 degrees from the localizer bearing when the APPR mode is selected, the CDI needle will have full deflection. The "V/L ARM" and "HDG" annunciators will be lighted, signifying that the navigation mode which follows VOR and localizer signals is armed but has not yet captured the localizer, and that the heading mode is active. The "LIN DEV" annunciator is not lighted, indicating that deflections on the CDI needle represent angular deviations when a localizer frequency is tuned.

The heading reference on the HSI is adjusted to select an aircraft heading that intersects the localizer bearing at an angle of 90 degrees or less. As the aircraft approaches the localizer bearing, CDI deflection decreases. When the deflection has decreased to a specified level, capture of the localizer bearing occurs, and the mode changes. The "V/L CAP" annunciator is lighted, and the "V/L ARM" and "HDG" annunciators are extinguished. Autopilot guidance will turn the aircraft to alignment with the localizer bearing, and will track the localizer to keep the CDI centered. Shortly after localizer capture, the "G/S ARM" annunciator will light, indicating that the glide-slope tracking circuit is armed.

Interception of the localizer should be planned to occur below the glide-slope. The glide-slope indicators on the ADI and HSI will normally be at full upward deflection at the time of localizer capture. As the autopilot guides the aircraft inbound along the localizer at constant altitude ("ALT HOLD" mode may be engaged), deflection of the glide-slope indicators will decrease. When the indicators reach the center, glide-slope capture will occur. The "G/S CAP" annunciator will light, and the "G/S ARM" annunciator will be extinguished. If the altitude hold mode was engaged before glide-slope capture, this mode will disengage, and the "ALT" annunciator will be extinguished. Vertical guidance circuits of the autopilot will follow the glide-slope while lateral guidance tracks the localizer, until the pilot selects the go-around mode, or disengages the autopilot for a manual landing.

BACK-COURSE MODE.

The back-course (B/C) mode is similar to the approach mode, but guides the aircraft to the opposite end of the runway on a course which is the reciprocal of the localizer runway bearing. No glide-slope guidance is available in the back-course mode.

Selection of the back-course mode reverses the response of the autopilot computer to CDI error, which is necessary to correct the reversed CDI indication that results from the reciprocal course. Capture of the localizer occurs in the same manner as in a normal front-course approach.

If the bearing of the aircraft is far from the localizer reciprocal when the back-course mode is energized, the "V/L ARM" and "HDG" annunciators will be lighted, and the CDI will have a large deflection. The heading reference can be selected on the HSI to provide a heading that intersects the localizer reciprocal at an angle of 90 degrees or less. As the aircraft approaches the reciprocal, CDI error will decrease. At a specified level, capture of the localizer reciprocal will occur, the "V/L CAP" annunciator will light, the "HDG" annunciator will be extinguished, and the aircraft will turn to alignment with the localizer runway bearing reciprocal.

GO-AROUND MODE.

The go-around mode provides autopilot control of a wings-level climb from a missed approach.

The go-around mode is engaged by pressing a button labeled "GA" on either control wheel. When this mode is energized, all other modes are cancelled, and the go-around indicator light on the ADI is lighted. The guide bars move to a wings-level and nose-up position representing a normal climb attitude. The pilot must also apply engine power at the time of engaging the go-around mode, so that the aircraft will climb and not stall.

The go-around mode provides autopilot control of the proper climbing attitude of the aircraft while the pilot devotes attention to setting power, retracting landing grear and flaps, and any other tasks required in establishing the go-around. After the climbing situation has stabilized, the pilot can select another mode, such as heading, to direct the aircraft to the missed-approach point. Selection of another mode, or pressing the CWS button, cancels the go-around mode.